EUROPEAN ORGANIZATION FOR NUCLEAR RESEARCH

CERN-EP/90-13
23 January 1990

THE ACCURACY OF HEAVY ION MASS MEASUREMENTS
USING TOF-ICR IN A PENNING TRAP*

G. Bollen[1,2], R. B. Moore[2,3], G. Savard[1] and H. Stolzenberg[1]

[1] *Institut fur Physik, Universitat Mainz, Mainz, Fed. Rep. Germany*
[2] *CERN, Geneva, Switzerland*
[3] *Foster Radiation Laboratory, McGill University, Montreal, Canada*

Abstract

Ion motion in a Penning trap and the electrical signals it can produce has been analyzed for the purpose of identifying the important causes of uncertainty in high accuracy mass measurements of heavy ions. The role of the azimuthal quadrupole electric field in signal pick-up, and its effects on ion motion at the sum frequency of the cyclotron and the magnetron motions, has been identified. A useful scheme for calculating the signal strength and the strength of the interaction between an applied field and the ion motion has been developed. The important sources of uncertainty in using the sum frequency of the cyclotron and magnetron motions for determining the ion mass are discussed. Particular application is made to the case of cyclotron resonance detection by observation of the time of flight (TOF) of ejected ions.

Submitted for publication to the Journal of Applied Physics

* This publication comprises part of the thesis of G. Bollen.

I. INTRODUCTION

The Penning trap has become a widely used device for high resolution mass spectrometry using ion cyclotron resonance (ICR).[1] Resolutions of over 4×10^8 have been achieved.[2] However, for accurate absolute mass determinations, this technique has not yet supplanted traditional fly-through spectrometers based on accurately established electric and magnetic fields. For example, the Smith spectrometer has given accuracies which have reached 1 part in 10^9, even though it has a resolution usually of only several hundred thousand.[3] This compares to typical accuracies of 70 ppm[4] or, with extreme care in calibration, 1 ppm[5] for ion cyclotron resonance in Penning traps.

The high precision to which modern Penning trap parameters can be established and the high stability of the devices should make them useful for high accuracy measurements. Van Dyck, Schwinberg and Dehmelt[6] have dramatically demonstrated the possibilities by their work on a single electron in a Penning trap (which they have called "Geonium"). The accuracy of their measurement of the magnetic moment of the electron, 4 parts in 10^{12}, is about 900 times better than previous measurements by other techniques. Wineland et al[7] have predicted that accuracies of mass measurements near 1 part in 10^{13} should be possible.

With modern high-homogeneity superconducting solenoids, the principle source of inaccuracies in ICR mass spectrometry in a Penning trap are uncertainties about the electric field experienced by the ions in the trap. The effect of this electric field on the motion of charged particles in a Penning trap was first called to attention by Sommer, Thomas and Hipple in 1951[8] in a paper describing the use of their invention, the Omegatron,[9] to determine e/m by Ion Cyclotron Resonance. Qualitatively, the radially repulsive electric field experienced by an ion cancels some of the Lorentz force due to the magnetic field. The actual cyclotron frequency of the ion is therefore reduced from the cyclotron frequency the ions would have if there were no electric field, i.e. $(q/m)B \equiv \omega_c$. Nevertheless, a collection of ions of a specific type given a specific electrical impulse to set up a coherent motion will have a very definite cyclotron frequency for that coherent motion. They will therefore produce a highly resolved signal of very precise frequency. Accurate mass determination requires a knowledge of how much the electric field causes this precise frequency to deviate from the value ω_c.

The electric field experienced by an ion in a Penning trap can be usefully considered to have two origins; the voltage applied to the electrodes forming the trap and the space charge of the ion cloud. The first published analysis of the effect of the applied electric field on charged particle motion in a Penning trap was by Byrne and Farago.[10] The effects of the space charge are more difficult to evaluate.[11] The key to the success reported in ref. 5 was the use of a single charged particle with its motion cooled so as to be very near the center of a precisely constructed trap. This, of course, completely removes the effects of the space charge field leaving only the uncertainties about the effects of the electric field of the applied voltage and about the magnetic field, both of which are reduced by limiting the extent of the motion.

In this paper, we present an analysis of the motion of heavy ions in a Penning trap and the interaction between this motion and a circuit connected to the electrodes of the trap from the point of view of obtaining high accuracy in mass determinations by ICR. The starting point of our investigations is the very thorough review article by Brown and Gabrielse[12] which presents the type of analysis of a Penning trap that is required for high accuracy work. Their paper concentrates on the parameters of importance in working with electrons. Our paper presents an analysis aimed for high accuracy mass measurement of heavy ions. We will follow closely the methods developed in Ref. 12 and will use the symbols and some of the equations of that work.

II. ION MOTION IN AN IDEAL PENNING TRAP

The solution of Laplace's equation for the electric field for a set of electrodes forming a Penning trap are most conveniently expressed in spherical coordinates r, θ, φ,

$$\phi = \sum_{lm} a_{lm} \phi_{lm} \tag{1}$$

where

$$\phi_{lm} = r^l P_l^m(\cos\theta) \cos m\varphi \tag{2}$$

and $P_l^m(\cos\theta)$ are the associated Legendre polynomials.

For a trap which has electrode symmetry about a median plane perpendicular to an axis, only the even powers of l will contribute. For azimuthally uniform potentials ($m = 0$) only the normal Legendre polynomials $P_l(\cos\theta)$ contribute. The lowest order of these ($l = 0$) is, of course, that of a uniform potential which is of no interest. The next lowest even order is the quadrupole;

$$\phi_2 = a_2 \, r^2 P_2(\cos\theta) \tag{3}$$

which can be expressed in its more familiar form in cylindrical coordinates r, z, φ;

$$\phi_2 = \frac{a_2}{2} \left(2z^2 - r^2 \right) \tag{4}$$

Such a potential can be set up by electrodes which follow the two hyperboloids of revolution specified by

$$z^2 - \frac{r^2}{2} = \pm z_0^2 \tag{5}$$

where z_0 is half the distance between the two end electrodes. If the voltage of the end electrodes relative to the ring is V_0, then the coefficient for the quadrupole term can be conveniently expressed as

$$a_2 = \frac{V_0}{2z_0^2} \tag{6}$$

This quadrupole field is very important for Penning traps because of its simplicity;

$$E_r = a_2 r \quad ; \quad E_z = -2a_2 z \tag{7}$$

This electric field has three effects on ion motion. It not only provides the restoring force on the ion that confines the axial motion to oscillations at an angular frequency ω_z but it also modifies the cyclotron frequency as already mentioned above and in addition introduces a third type of motion; a slow magnetron precession. In the pure quadrupole field, these three motions are completely independent oscillations with the following angular frequency relationships;

$$\omega_{\pm} = \frac{\omega_c}{2} \pm \sqrt{\left(\frac{\omega_c}{2}\right)^2 - \frac{\omega_z^2}{2}} \tag{8}$$

where ω_c is the unperturbed cyclotron frequency $(q/m)\,B$, ω_+ is the reduced cyclotron frequency, ω_- is the magnetron frequency and the axial angular oscillation frequency ω_z is given by

$$\omega_z^2 = 2\frac{q}{m}a_2 \tag{9}$$

The relationship between these three fundamental frequencies of ion motion in a Penning trap are more clearly seen by noting that

$$\omega_+ + \omega_- = \omega_c \tag{10a}$$

$$\omega_+\omega_- = \frac{\omega_z^2}{2} \tag{10b}$$

or that

$$\omega_+^2 + \omega_-^2 + \omega_z^2 = \omega_c^2 \tag{11}$$

Eqn (10) is a very important consequence for accurate mass measurements in Penning traps. It means that while ω_c cannot be observed directly, it can be determined by observing the individual frequencies ω_+ and ω_- or by observing the sum signal of the $\omega_+ + \omega_-$ motions if it is generated by the system.

III. THE DETECTION OF ION MOTION IN A PENNING TRAP

A. The signal induced by ion motion

Ion motion in a Penning trap is usually detected by having the motion induce an electrical signal between electrodes forming the trap. Simple models of the interaction between ions and electrodes in geometries such as those of a Penning trap have been introduced by Marshall and Comissarow[13], by Wineland and Dehmelt[14] and by Schweikhard et al.[15] Here we will develop a more comprehensive treatment which is applicable to a wide variety of possible geometries.

An ion of charge q moving in an electric field $\boldsymbol{E}$ at velocity $\boldsymbol{v}$ absorbs energy from the field at the rate $q\boldsymbol{v}{\cdot}\boldsymbol{E}$. If the electric field is due to a potential difference V applied to a set of electrodes and the energy is replaced by the circuit applying the potential difference (Fig. 1), then the current supplied by this circuit is given by

$$i = \frac{q\boldsymbol{v}{\cdot}\boldsymbol{E}}{V} \tag{12}$$

The electric field $\boldsymbol{E}$ is, of course, proportional to V and so the current i is

$$i = q\boldsymbol{v}{\cdot}\boldsymbol{E}_1 \tag{13}$$

where $\boldsymbol{E}_1$ is the unit electric field or that which would be caused by a 1 volt potential difference on the electrodes.

An ion in a trap will typically undergo oscillatory motion in one or more coordinates. For any one of these oscillatory motions, there will be a corresponding oscillatory current in an external circuit. As shown in Ref. 12, the ion motion can be treated as an equivalent lumped series LC circuit shorting the electrodes, the inductance of this circuit being associated with the kinetic energy of the ion motion;

$$\text{Kinetic energy} = \frac{1}{2}mv^2 = \frac{1}{2}Li^2 \; ; \; L = \frac{mv^2}{i^2} = \frac{mv^2}{(q\boldsymbol{v}{\cdot}\boldsymbol{E}_1)^2} \tag{14}$$

which, for the simple case of an ion moving parallel to the uniform electric field between two infinite parallel plates of separation d, gives

$$L = \frac{md^2}{q^2} \tag{15}$$

The equivalent capacitance is associated with the potential energy of the ion in the confining electric (magnetic) field and is related to the equivalent inductance through the free oscillation angular frequency ω;

$$C = \frac{1}{\omega^2 L} \tag{16}$$

It can be immediately seen that the ion motion presents a source of very high electrical impedance. For a mass 100 ion between two plates separated by 1 cm, the equivalent inductance is about 6×10^6 H. An oscillation of 1 MHz therefore presents an impedance of about $4 \times 10^{13}\ \Omega$.

This high impedance is related to the small effect that the voltages produced by the ion motion have on the ion motion itself. Another aspect of this phenomenon can be seen through the concept of the Q of the ion-electrode system. If the external circuit presents a simple resistance to the ion motion, then the energy of the ion motion (or its equivalent resonant circuit) is, of course, dissipated through this resistor R. The Q of the total circuit will then be $\omega L/R$. For a singly charged ion of mass number $A = 100$ between electrodes that can be approximated as parallel planes with $d = 1$ cm and undergoing oscillatory motion at $\omega = 10^6$, the Q of the system for $R = 1\ \text{M}\Omega$ will be about 6×10^8 corresponding to a decay time constant of about 1000 s. For a collection of ions, the Q will be inversely proportional to the number of ions undergoing a coherent oscillation and so, for 6000 ions undergoing such a coherent motion, will drop to about 10^5 and a decay time of 0.16 s.

In a typical circuit connected to electrodes of a trap, there will be a complex admittance associated with the capacitance C and any external tuning inductance L which parallels a simple passive resistor R. The resulting signal level will therefore depend on the admittance of this circuit;

$$V_s = \frac{i}{Y} = qv \cdot E_1 \frac{1}{\frac{1}{R} + i\omega C - \frac{1}{i\omega L}} \tag{17}$$

The problem of determining the signal that will appear in an external circuit due to a given ion motion in a trap, or the effect of a driving voltage from an external circuit on that motion, is therefore that of determining $v \cdot E_1$. The velocity v is determined by analyzing the ion motion in the trap which is itself influenced by the electric field. The unit electric field E_1 is determined by the electrode configuration.

analyzing the ion motion in the trap which is itself influenced by the electric field. The unit electric field E_1 is determined by the electrode configuration.

B. The electric fields from detection electrodes in a Penning trap

Because the determination of cyclotron and magnetron motion involves azimuthal velocity components, the electrode configurations will, in general, not have azimuthal uniformity. For example, the common method for detecting cyclotron motion is to have the ring electrode split into two halves in a plane through the axis. Such an electrode configuration introduces potential components with all the odd values of m in Eqn. (1), the most dominant being, of course, the dipole ($m = 1$)

What is required for any such given electrode configuration is to evaluate the m^{th} order field components

$$\phi_m(r,z) = \sum_l a_{lm} r^l P_l^m(\cos\theta) \tag{18}$$

whereupon the potential can be expressed as

$$\phi = \sum_m \phi_m \sin m\varphi \tag{19}$$

where the azimuthal phase factors for ϕ_m are buried in the coefficients a_{lm}. For a symmetry in which ϕ is antisymmetrical in φ, a_{lm} will all be real.

Laplace's equation for these multipoles is generally most conveniently expressed in cylindrical coordinates;

$$\frac{1}{r}\frac{\partial}{\partial r}\left(r\,\frac{\partial\phi_m(r,z)}{\partial r}\right) + \frac{\partial^2\phi_m(r,z)}{\partial z^2} - \frac{m^2\phi_m(r,z)}{r^2} = 0 \tag{20}$$

Unfortunately, for values of $m \neq 0$, this equation does not have simple analytical solutions even for electrodes that are hyperboloids of revolution. In principle, the ϕ_m components for any electrode configuration can be determined numerically by a variety of techniques, the usual for complex geometries being that of computation by relaxation or finite element methods. However, the electric fields in a trap are three dimensional and this generally makes a specific configuration very costly to calculate. A great simplification is achieved if the electrode geometry has azimuthal symmetry, (i,e. uniform radius at any given z). The electrode geometry is then defined by a specific r,z contour and, if the potential along this r,z contour at any given ϕ can be made to vary as $V_{o_m} \sin m\phi$, then one has the boundary conditions to create the specific m^{th} multipole.

In principle, such a boundary condition could be set up by having the electrodes made up of an infinite set of wires following a uniform r,z contour but of potentials $V_{o_m} \sin m\phi$. In practice the electrodes can be made to follow a specific r,z contour but will have finite azimuthal extent. An example is the case already mentioned of the hyperboloidal ring of a Penning trap split into two equal segments through the $\phi = 0$ plane with potentials $\pm V$ applied to the two halves in order to excite or detect cyclotron motion. Such a boundary condition can be decomposed into Fourier components giving all the odd multipoles according to

$$V_{o_m} = \frac{4}{\pi}\frac{V}{m} \quad (m \text{ odd}) \tag{21}$$

For a given r,z contour of the electrodes, the potential distribution for any of these component multipoles can then be solved by a two-dimensional relaxation of (20). For a square grid, the simple relaxation evaluation of the potential ϕ_o at a point j grid steps from the axis, in terms of the surrounding values of ϕ, is

$$\phi_o = \frac{(\phi_1 + \phi_2 + \phi_3 + \phi_4) + \dfrac{(\phi_1 - \phi_3)}{2j}}{4 + \left(\dfrac{m}{j}\right)^2} \tag{22}$$

where ϕ_1, ϕ_2, ϕ_3 and ϕ_4 are the potentials of the surrounding points clockwise from the radially outward point. This simple relaxation can easily be adapted to the usual techniques of over-relaxation and Chebychev acceleration.[16] For the case of $m = 0$, one has the standard relaxation in cylindrical coordinates with the symmetry condition that the radial gradient of the potential at the axis must be zero. For the cases of $m \neq 0$, the symmetry condition leads to the potential along the axis being uniformly zero.

The azimuthal multipole components for electrodes with non-azimuthally symmetrical geometry, such as the cubic configuration commonly used in FT-ICR mass spectroscopy, are not so easily determined. In such cases, a full three dimensional relaxation has to be performed (usually best in cartesian coordinates) and the multipole components evaluated by a Fourier type decomposition of the results. In any case, such geometries can be expected to have large deviations from the ideal Penning trap electric field and therefore not be suitable for high accuracy mass determinations.

We have modified a simple relaxation program for cylindrical geometry to that required for (22). Solving the dipole case for electrodes which are hyperboloids of revolution with the ring electrode having an azimuthal voltage component for $m = 1$ of V_{o_1} and the end electrodes both at ground, we have obtained an electric field distribution which can be approximated to third order by

$$E_x = -2cxy \ ; \ E_y = -a - c(3y^2 + x^2 - 4z^2) \ ; \ E_z = 8cyz$$

$$a = 0.73 \times \frac{V_{o_1}}{r_o} \quad ; \quad c = 0.29 \times \frac{V_{o_1}}{r_o^3} \tag{23}$$

where r_o is the inner radius of the ring electrode. The effect of the shielding of the end electrodes is to reduce the dipole electric field in the trap center to 0.73 of that for the same azimuthal voltage variation on a long cylinder.

For the same electrode configuration but with an azimuthal quadrupole field caused by a voltage component V_{o_2}, we have found that the solution can be approximated to third order by

$$E_x = -2by - 2dy^3 - 6d(x^2y - 2yz^2)$$

$$E_y = -2bx - 2dx^3 - 6d(xy^2 - 2xz^2)$$

$$E_z = 24dxy\,z$$

$$b = 0.80 \times \frac{V_{o_2}}{r_o^2} \qquad d = 0.16 \times \frac{V_{o_2}}{r_o^4} \tag{24}$$

Again, the solution shows the expected quadrupole field variation at the center of the trap but with the shielding effect of the end electrodes being 0.80.

Finally, the solution for the sextupole field ($m = 3$) can be approximated to third order by

$$E_x = -6cxy \ ; \quad E_y = -3c(y^2 - x^2); \quad E_z = 0$$

$$c = 0.85 \times \frac{V_{o_3}}{r_o^3} \tag{25}$$

As an example of a real situation, the split ring electrode potential described by (21) will produce a total unit electric field

$$E_{1_x} = -2.90 \frac{1}{r_o^3} xy$$

$$E_{1_y} = -0.93 \frac{1}{r_o} + \frac{1}{r_o^3}(1.45x^2 - 0.03y^2 + 1.48z^2)$$

$$E_{1_z} = 2.95 \frac{1}{r_o^3} y\,z \tag{26}$$

For a ring electrode split into 4 equal quadrants and with potentials $\pm V$ applied in quadrupole fashion to these quadrants, the unit electric fields, to third order, are

$$E_{1_x} = -2.0\,\frac{y}{r_0^2} + \frac{1}{r_0^4}\left(-1.22\,x^2y - 0.40\,y^3 + 2.44\,yz^2\right)$$
$$E_{1_y} = -2.0\,\frac{x}{r_0^2} + \frac{1}{r_0^4}\left(-0.40\,x^3 - 1.22\,xy^2 + 2.44\,xz^2\right)$$
$$E_{1_z} = 4.9\,\frac{xyz}{r_0^4} \qquad (27)$$

C. Signals induced by cyclotron motion in azimuthal multipole fields

From the results of the previous section, the signal induced in various electrode configurations of the Penning geometry can be determined. The signal for the z motion in a circuit connected to the end electrodes has already been discussed elsewhere[14]. What will be discussed here is the signal due to the cyclotron motion in a circuit which produces an azimuthal multipole field in the mid-plane of the trap.

The simplest such circuit is one connecting the end electrodes, at a common potential, to a ring at uniform potential. The field produced is, of course, a modulation of the trapping field ($m = 0$). The current source $qv \cdot \boldsymbol{E}_1$ for cyclotron motion in such a field can be easily obtained. The cyclotron motion, a linear combination of a reduced frequency cyclotron motion of radius ρ_+ at ω_+ and of magnetron motion of radius ρ_- at ω_- is;

$$x = \rho_+ \cos\omega_+ t + \rho_- \cos\omega_- \tau$$
$$y = \rho_+ \sin\omega_+ t + \rho_- \sin\omega_- \tau$$
$$v_x = -\rho_+\omega_+ \sin\omega_+ t - \rho_-\omega_- \sin\omega_- \tau$$
$$v_y = \rho_+\omega_+ \cos\omega_+ t + \rho_-\omega_- \cos\omega_- \tau \qquad (28)$$

where the ω_+ and ω_- motions are assumed to start in phase on the x axis. From (6) and (7), the unit electric field is

$$E_{1_x} = \frac{x}{2z_0^2} \qquad E_{1_y} = \frac{y}{2z_0^2} \qquad (29)$$

The signal current source is;

$$qv \cdot \boldsymbol{E}_1 = q(v_x E_{1x} + v_y E_{1y}) = \frac{q}{2z_0^2}\,\rho_+\rho_-(\omega_+ - \omega_-)\,\sin(\omega_+ - \omega_-)\,t \qquad (30)$$

The ion motion therefore induces a signal of frequency $\omega_+ - \omega_-$ and of amplitude given by the product of ρ_+, ρ_- and $\omega_+ - \omega_-$. In the limit of $\rho_+ << \rho_-$ (or $\rho_- << \rho_+$) this is easily seen to be reasonable; the signal induced in the ring electrode is due to the radial oscillation which has a frequency $\omega_+ - \omega_-$ and amplitude ρ_+ (or ρ_-) in a radial electric field which has magnitude proportional to ρ_- (or ρ_+). This signal in the basic electrodes of a Penning trap has been made use of in the so-called parametric-mode excitation .[17,18]

The signal induced by a dipole field in a circuit connected to the two halves of a split ring of a Penning trap is especially easy to calculate. From (26) this dipole component is

$$E_1 = E_{1_y} = -0.93\frac{1}{r_0} \tag{31}$$

For such a field the two cyclotron motions completely decouple to give signals at ω_+ and ω_-;

$$qv{\cdot}\boldsymbol{E}_1 = -0.93\frac{q}{r_0}(\rho_+\omega_+ \sin\omega_+ t + \rho_-\omega_- \sin\omega_-\tau) \tag{32}$$

The effect of the second order terms in (26) will be to introduce signals of the combinatorial frequencies made up of three frequencies from $\pm\,\omega_+, \pm\,\omega_-$, or one of these and $\pm\,2\omega_z$. Thus the combination frequency $\omega_+ + \omega_-$ is not seen for this electrode configuration. From symmetry considerations, neither will it be seen for any higher odd order *m* component of electric field.

However, a signal of frequency $\omega_+ + \omega_-$ will arise in an azimuthal quadrupole field. Here (27) and (28) lead to

$$qv{\cdot}\boldsymbol{E}_1 = 2.0\frac{q}{r_0^2}[\rho_+^2\,\omega_+ \cos 2\omega_+ t + \rho_-^2\,\omega_- \cos 2\omega_- t + \rho_+\rho_-(\omega_+ + \omega_-)\cos(\omega_+ + \omega_-)\,t\,] \tag{33}$$

Thus the strongest signals in a circuit connected in a quadrupole configuration to a ring electrode split into 4 quadrants would be of frequencies $2\omega_+$, $2\omega_-$ and $\omega_+ + \omega_-$. These signals have indeed been seen in a quadrupole configuration for the ring electrode of a Penning trap.[19]

The double frequency signals are clearly due to the 2 cycles of potential seen by a particle undergoing pure ρ_+ or ρ_- motion. The $\omega_+ + \omega_-$ signal can perhaps be visualized most easily by noting that, from the point of view of the ion's position, the electric field direction for a static electric field will rotate backwards at the same rate that the magnetron motion moves forward.

Thus the desired $\omega_+ + \omega_-$ signal is directly obtained by a quadrupole configuration for the ring electrode of a Penning trap. However, this signal will be very low compared to the noise in a typical circuit. The amplitude of the signal current for a mass 100 ion in a magnetic field of 6 T and with radii of cyclotron and magnetron motions about 1/20 of z_0) will be about 5×10^{-15} A at 1 MHz. For a circuit with an input capacitance of 1 pF in parallel to an input resistance of 1 MΩ, the signal level will be about 5×10^{-10} V_{rms}. In such a circuit, the Johnson noise in a 1 Hz band (a 1 MHz signal resolved to 1 ppm) will be about 2×10^{-8} V_{rms}. Thus 250 ions would be needed to obtain a signal level equal to the noise level. From the considerations of section III-A it can be estimated that the decay time of the ion motion for 250 ions connected to such a circuit will be of the order of a few seconds. This signal to noise ratio could be improved with higher circuit resistance but this would also decrease the decay time of the motion making it impossible to obtain the same resolution. It appears that several hundred (heavy) ions is the practical lower limit for the number that can be observed from excitation of a passive circuit connected to the electrodes in a Penning trap.

It may be noted that the signal level for the cyclotron motion alone in a circuit connected in the dipole mode would be about 10 times larger then that for the quadrupole mode (due to the linear rather than the quadratic dependence of the signal on the ratio of cyclotron radius to z_0). However, the magnetron motion, which must then also be observed so as to determine the sum frequency, will have a considerably reduced signal level because of its much lower frequency.

It should also be noted that for a $\omega_+ + \omega_-$ signal to be generated by a collection of ions they must have both cyclotron and magnetron motions and these motions must individually have some coherency. This, however, is relatively easy to accomplish. The coherence in the magnetron motion can be produced by creating the ions with their center of mass at a finite trap radius. The coherence in the cyclotron motion can be produced, as in normal FFT-ICR mass spectrometry, by exciting the motion with a resonant dipole field (see section IV-A).

D. Detection of ion cyclotron resonance by TOF after ion ejection

The large number of ions needed to obtain a clearly resolved signal of cyclotron motion in a Penning trap, even at resolutions of 1 ppm, leads to the consideration of a scheme for detecting ion cyclotron resonance by observing ejected ions. Since destructive detection is quite feasible for even a single ion, such a scheme would make it possible to attain the goal of observing the effect of cyclotron resonance with only a single ion in the trap. Of course, to observe the full resonance and determine the frequency of the cyclotron motion, the observation has to be repeated many times at different driving frequencies scanning the cyclotron frequency. Such a measurement will generally take as many ions in total as that required in the one bunch for an FT-ICR observation. Furthermore, one loses the coherency in the ion motions which gives the highly resolved signal in FT-ICR, leading to a resolution which depends on ability to control the parameters of the ion motion and the trap. Nevertheless, by removing the different driving frequencies scanning the cyclotron frequency. Such a measurement will generally take as many ions in total as that required in the one bunch for an FT-ICR observation. Furthermore, one loses the coherency in the ion motions which gives the highly resolved signal in FT-ICR, leading to a resolution which depends on ability to control the parameters of the ion motion and the trap. Nevertheless, by removing the uncertainties about the space charge effects, such a scheme should be inherently more accurate than FT-ICR. It is also very attractive for the mass determination of radioactive ions which may be available at only a very low rate of production and which may have a half-life that prohibits their assembly into one collection in a Penning trap.

A system which observes cyclotron resonance in a Penning trap by external ion detection was first published by Gräff, Kalinowsky, and Traut[20]. The principal used is that a change in the motion of a charged particle resulting in a change in its magnetic potential energy can be detected by observing a change in the kinetic energy of the particle when it is ejected from the magnetic field. This idea was first published by Bloch[21] in a proposal of a scheme for a determination of the g-factor of an electron. In the case of the increased magnetic potential of an ion due to an enhanced cyclotron motion, the resulting increase in the kinetic energy of an ejected ion can be observed in the time of flight of the ion from the trap to a detector. As a representative example, a singly charged ion of mass 100 and with a cyclotron radius of 1 mm in a magnetic field of 6 T will have, after it is ejected into a magnetic field which is negligible, an axial kinetic energy of about 17 eV due to its original magnetic potential.

In Ref. 20, it was shown that it was possible to induce cyclotron motion by a resonance effect at $\omega_+ + \omega_-$. Using this resonance, the unperturbed cyclotron frequency ω_c of a proton in a field of about 6 T was determined to 0.05 ppm. This success inspired the construction of a similar system for absolute mass measurement of radionuclides at ISOLDE[22,23].

A special requirement of such a scheme for measuring radionuclides is that, because of their limited availablility, they must usually be delivered to the trap as ions from an outside source. In 1986 the first such transfer of ions into the Penning trap was reported[24], followed in 1988 by preliminary results on the measurement of several radioactive nuclides[25-28].

The original system installed at ISOLDE was meant to prove the feasibility of the method and to assess the significant design parameters for achieving high accuracy absolute mass measurements in such an environment. As such, it has not only given new mass measurements of radionuclides but has served as a very useful test-bed for absolute mass measurements in such an environment. As such, it has not only given new mass measurements of radionuclides but has served as a very useful test-bed for our analysis of ion motion in Penning traps. In the remainder of this paper we will refer to that system as an example.

The mechanism by which cyclotron motion can be excited by applying an oscillatory electric field at frequency $\omega_+ + \omega_-$ is of primary importance in the analysis of the system. It was recognized by the original developers of the system used in ref. 20 that the required coupling of the cyclotron and magnetron motion can not be induced by the dipole field of the split ring; that it must arise from some higher order coupling terms.[29] We have therefore undertaken a more general analysis of the excitation of cyclotron and magnetron motions in a Penning trap by applied azimuthal multipole fields.

IV. EFFECTS OF ELECTRODE EXCITATION ON ORBIT MOTION

To analyze the effect of applied oscillating electric fields on the ion orbit motions, it is most convenient to express the motion by the velocity vectors V^+ and V^- as used in Ref. 12;

$$V^+ = \dot{r} - \omega_- \hat{z} \times r$$

$$V^- = \dot{r} - \omega_+ \hat{z} \times r \qquad (34)$$

where r and $\dot{r}$ are the position and velocity vectors of the ion and $\hat{z}$ is the unit vector on the z axis. V^+ and V^- are the velocities in coordinate systems which are moving with velocities $\omega_- \hat{z} \times r$ and $\omega_+ \hat{z} \times r$ respectively. The meaning of these velocity vectors is most easily seen in the special cases of only cyclotron or magnetron motion. They then become

$$V^+ = (\omega_+ - \omega_-)\, \hat{z} \times r$$

$$V^- = 0 \qquad (35a)$$

and

$$V^- = -(\omega_+ - \omega_-)\, \hat{z} \times r$$

$$V^+ = 0 \qquad (35b)$$

where it can be seen that, since $\omega_+ > \omega_-$, V^- rotates backwards relative to V^+ and to the cyclotron and magnetron motions themselves (which both rotate forwards).

The advantage of these velocity vectors lies in the Hamiltonian for the radial and azimuthal motion in a pure cylindrical quadrupole Penning trap taking on an especially simple form

$$H = \frac{1}{2} m \, \frac{\omega_+ {V^+}^2 - \omega_- {V^-}^2}{\omega_+ - \omega_-} \qquad (36)$$

with the canonical angular momentum becoming

$$p = \frac{m}{2} \left(V^+ + V^- \right) \qquad (37)$$

showing that the equations of motion in $\mathbf{V}^{+}$ and $\mathbf{V}^{-}$ are completely decoupled. They are

$$\dot{V}^{\pm} = \omega_{\pm}\hat{z}\times V^{\pm} \tag{38}$$

It is easily seen from the form of the Hamiltonian that the energy in the magnetron motion is negative, as indeed it must be since the negative electrical potential on a magnetron orbit is numerically greater then the kinetic energy of the ion. This also has the implication that, in the Hamiltonian formalism which is important in the quantum mechanical formulation of the energy states of "Geonium" as developed in Ref. 12, the frequency of the magnetron motion is negative.

An applied electric field added to the equations of motion (38) gives

$$\dot{V}^{\pm} = \omega_{\pm}\hat{z}\times V^{\pm} + \frac{q}{m} E(r,t)$$

or, in component form

$$\begin{aligned} \dot{V}_x^{\pm} &= -\omega_{\pm} V_y^{\pm} + \frac{q}{m}E_x \\ \dot{V}_y^{\pm} &= \omega_{+} V_x^{\pm} + \frac{q}{m}E_y \end{aligned} \tag{39}$$

A. The effect of a driving azimuthal dipole electric field

For a driving dipole electric field the two sets of equations in V^{+} and V^{-} are completely decoupled and can be solved independently. For an oscillating dipole $E_y = E_d \sin \omega_d t$ (where, in (23), $E_d = -a$), the stable solutions for both V^{+} and V^{-} are elliptical orbits;

$$V_x^{\pm} = C_1 \cos \omega_d t$$
$$V_y^{\pm} = C_2 \sin \omega_d t$$

$$C_1 = \frac{\omega_d}{\omega_{\pm}} B \;;\; C_2 = -\frac{\omega_{\pm}^2}{\omega_{\pm}^2 - \omega_d^2}\frac{q}{m}E_d \tag{40}$$

Thus the coordinates of both motions behave as simple oscillators and there will be no resonance effect at $\omega_+ + \omega_-$. For a driving field of frequency ω_d applied for a time T_{rf} to a stationary particle at the center of a trap, the energy in a motion of frequency $\omega_\pm$ at the end of this period will be given by the Fourier transform;

$$I(\omega) \;\alpha\; \frac{\sin^2\left(\frac{\omega_d - \omega_\pm}{2} \times T_{rf}\right)}{\left(\frac{\omega_d - \omega_\pm}{2}\right)^2} \tag{41}$$

This response function is shown in Fig. 2. Defining $\Delta\omega$ as $\omega_d - \omega_\pm$, the half height of this function occurs at $\sin^2(\Delta\omega T_{rf}) = (\Delta\omega)^2/8$. Defining the resolution as the FWHM of this function and expressing it in terms of the cycle frequency gives

$$R \approx 0.89\, \nu_\pm T_{rf} \tag{42}$$

Thus the individual frequencies $\nu_\pm$ can be determined by two separate dipole excitations and the results added to give the required sum frequency. However, the system does not respond directly to an excitation at this sum frequency. Such a response must therefore come from higher order azimuthal multipoles.

B. The effect of a driving azimuthal quadrupole electric field

A driving azimuthal quadrupole field is of interest in that in section III-C it was shown that a passive azimuthal quadrupole field in a Penning trap produces a signal with a frequency component $\omega_+ + \omega_-$. It is therefore expected that a driving azimuthal quadrupole field will produce a "resonance" effect at this frequency.

The equations of motion with an applied azimuthal quadrupole field of the form (24) become

$$\begin{aligned} \dot{V}_x^\pm &= -\omega_\pm V_y^\pm - 2\frac{q}{m} by \\ \dot{V}_y^\pm &= \omega_\pm V_x^\pm - 2\frac{q}{m} bx \end{aligned} \tag{43}$$

To solve these equations, the coordinates x and y must be expressed in terms of V^+ and V^- . From the defining equations (34) it can be shown that the needed relations are

$$x = -\frac{V_y^+ - V_y^-}{\omega_+ - \omega_-} \quad ; \quad y = +\frac{V_x^+ - V_x^-}{\omega_+ - \omega_-} \tag{44}$$

The equations (43) then become

$$\dot{V}_x^\pm = -\ \omega_\pm V_y^\pm + kV_x^+ - kV_x^-$$
$$\dot{V}_y^\pm = +\ \omega_\pm V_x^\pm - kV_y^+ + kV_y^-$$

$$k = -\frac{q}{m}\frac{2b}{\omega_+ - \omega_-} \tag{45}$$

Oscillating the quadrupole field at ω_d makes k an oscillatory term which may be conveniently expressed as $k = k_0 \cos \omega_d t$. This driving term now couples the two motions V^+ and V^-, a phenomenon analogous to the coupling of the states of a two-state atomic system by an oscillating electric field and which produces an oscillation in the populations of the two states. In this quantum mechanical effect, the population oscillation frequency is proportional to the coupling field strength.

Looking for a similar solution for the two cyclotron motions in a Penning trap, the possible solutions may be most conveniently expressed in exponential form as

$$V^\pm = A^\pm(t)\, e^{\pm i\omega_\pm t} \tag{46}$$

where $A^\pm(t)$ are assumed to be slowly changing amplitude functions and where note is taken that the V^- motion has negative rotation.

Expressing the cosine in the quadrupole driving term in exponential notation and dividing by common exponential factors in the equations gives the following form for the equations of motion;

$$\dot{A}_x^\pm \pm i\,\omega_\pm A_x^\pm$$
$$= -\ \omega_\pm A_y^\pm \pm \frac{k_0}{2}[A_x^\pm(e^{i\omega_d t} + e^{-i\omega_d t}) - A_x^\mp(e^{i(\omega_d - \omega_0)t} + e^{-i(\omega_d + \omega_0)t})]$$

$$\dot{A}_y^\pm \pm i\,\omega_\pm A_y^\pm$$
$$= -\ \omega_\pm A_x^\pm \pm \frac{k_0}{2}[A_y^\pm(e^{i\omega_d t} + e^{-i\omega_d t}) - A_y^\mp(e^{i(\omega_d - \omega_0)t} + e^{-i(\omega_d + \omega_0)t})]$$

$$\omega_0 = \omega_+ + \omega_- \tag{47}$$

For $\omega_d \approx \omega_o$ and k_o small ($<< \omega_-$), these equations show the possibility of slowly varying amplitudes to V^+ and V^- upon which are superimposed small high frequency oscillations of frequencies $\approx \omega_d$ and $2\omega_d$. The low frequency components of the equations give

$$\dot{A}_x^{\pm} = \mp\, i\, \omega \pm A_x^{\pm} - \omega \pm A_y^{\pm}(t) \mp \frac{k_o}{2} A_x^{\mp}\, e^{i(\omega_d - \omega_o)t}$$

$$\dot{A}_y^{\pm} = \mp\, i\, \omega \pm A_y^{\pm} - \omega \pm A_x^{\pm}(t) \mp \frac{k_o}{2} A_y^{\mp}\, e^{i(\omega_d - \omega_o)t} \qquad (48)$$

Assuming circular orbits and again taking into account that V^- rotates backwards gives

$$A_y^{\pm} = \mp\, i\, A_x^{\pm} = \mp\, i\, A^{\pm} \qquad (49)$$

and gives (48) the form

$$\dot{A}^{\pm} = \mp \frac{k_o}{2} A^{\mp}\, e^{\pm i(\omega_d - \omega_o)t} \qquad (50)$$

For $\omega_d = \omega_o$, the solution of these equations has the simple form

$$A^{\pm} = A_o^{\pm}\, e^{\pm i(\xi_{\pm} t + \varphi_{\pm})} \qquad (51)$$

with the conditions that

$$\xi_+ \xi_- = \left(\frac{k_o}{2}\right)^2 \; ; \quad \frac{\xi_+}{\xi_-} = \frac{A_o^+}{A_o^-}\, e^{2i((\xi_- - \xi_+)t + \varphi_- - \varphi_+)} \qquad (52)$$

For $\xi_{\pm}$ to be constants, meaning steady state solutions, then

$$\xi_+ = \xi_- = \pm \frac{k_o}{2} \; ; \; \varphi_+ = \varphi_- \pm \frac{\pi}{2} \qquad (53)$$

Any solution of (50) can be expressed as a linear combination of these steady state solutions;

$$A^+ = \alpha_1\, e^{i(\frac{k_o}{2}t + \varphi_- + \frac{\pi}{2})} + \alpha_2\, e^{i(-\frac{k_o}{2}t + \varphi_- - \frac{\pi}{2})}$$

$$A^- = \alpha_1\, e^{i(\frac{k_o}{2}t + \varphi_-)} + \alpha_2\, e^{i(-\frac{k_o}{2}t + \varphi_-)} \qquad (54)$$

Considering only the x components of the velocity variables, (54) become

$$V_x^+ = \alpha_1 \, e^{i((\omega_+ + \frac{k_o}{2})t + \varphi_- + \frac{\pi}{2})} + \alpha_2 \, e^{i((\omega_+ - \frac{k_o}{2})t + \varphi_- - \frac{\pi}{2})}$$

$$V_x^- = \alpha_1 \, e^{-i((\omega_- - \frac{k_o}{2})t - \varphi_-)} + \alpha_2 \, e^{i((\omega_- + \frac{k_o}{2})t - \varphi_-)} \qquad (55)$$

The combinations with $\alpha_1 = \pm \; \alpha_2$ are of particular interest in that these represent beating motions with a beat frequency of k_o. In such a circumstance an initial motion which is completely magnetron will convert completely into cyclotron motion and back, the time taken for the conversion from one to the other being

$$T_{\omega_- \to \omega_+} = \frac{\pi}{k_o} \qquad (56)$$

This phenomenon can be clearly seen in Fig. 3 which is obtained from a numerical integration of the equations of motion (43). For this figure, the quadrupole field strength relative to the magnetic and electric fields of the trap was chosen to give a complete transition from initial magnetron motion to cyclotron motion in about 60 cyclotron orbits.

Thus there is a situation in a Penning trap with azimuthal quadrupole excitation of the ion motion which is indeed analogous to the coupling of a two quantum state electron system by an applied electromagnetic field. There is little doubt that this is the mechanism by which the sum frequency $\omega_+ + \omega_-$ enhanced the cyclotron motion in the apparatus as described in ref. 20 and as in the ISOLDE apparatus. Equations (24), (45) and (56), and the approximation $\omega_+ - \omega_- \approx \omega_c$, together with the amplitude of V_{o_2} being $4/\pi$ of the amplitude V of an applied quadrupole potential to a set of quadrants, gives the applied potential required to completely convert magnetron to cyclotron motion as

$$V \approx 0.6 \, \frac{\pi}{T} \, B r_o^2 \qquad (57)$$

For a conversion time of 1 s in a trap with $r_o = 1$ cm in a field of 6 T, the required voltage is about 1 mV. This compares with voltages of the order of 100 mV apparently used in ref. 20 and of about 50-mV for the ISOLDE apparatus when used in a dipole excitation mode. When using a quadrupole excitation in the ISOLDE apparatus we have found that only about 0.7 mV is required for an equivalent enhancement of the cyclotron motion. It is easy to believe that the excitation in the dipole electrode configuration is due to a quadrupole component arising from mechanical and electrical asymmetries.

C. Resolution using quadrupole coupling of orbit motions

The detection of the phenomenon of coupling of the magnetron and cyclotron motion by a quadrupole field involves the scanning of the frequency of this field over the sum frequency $\omega_+ + \omega_-$. The qualitative effect is that, at frequencies deviating from the resonance, the driving field will not have time to complete the motion transform before it moves out of the proper phase relationship for achieving this transform. Thus a high field strength which completes this transform in a shorter time will allow a broader range of frequencies to satisfactorily complete the transform. For complete transformation of the magnetron motion to cyclotron motion, the frequency width of the response of the system is therefore inversely proportional to the time required for this transform.

To obtain the proportionality constant between the frequency width and the transfer time, (43) was numerically integrated for cases when $\omega_d \neq \omega_0$. The results are shown in Fig. 4.

As might be expected, it is seen that the FWHM of the response function for field strengths near a_{max} is about $1/T_{rf}$, where T_{rf} is the time of application of the quadrupole field. Defining this frequency width as the resolution of the system gives the simple relation

$$\text{Resolution} = f_c \times T_{rf} \qquad (57)$$

D. The effect of higher azimuthal multipole driving electric fields

It has been shown above that an observation of the $\omega_+ + \omega_-$ frequency can be made by using an azimuthal quadrupole configuration for the ring electrode of a Penning trap, both in FT-ICR spectroscopy and in ICR-ion ejection detection schemes. It is interesting to consider the possibilities of even higher azimuthal multipoles.

From symmetry considerations $\omega_+ + \omega_-$ frequency should appear for any even-order $2m$ multipole (m ≥ 2, even), the actual lowest frequency in which it appears being $(m/2)(\omega_+ + \omega_-)$. The octupole ($m = 4$) excitation would be obtained by a ring split into octants. The multipoles with $m/2$ having an odd value are especially interesting since, by Fourier decomposition of the boundary conditions as in (21) for a ring split into quadrants, they will be present to a degree in inverse proportion to $m/2$.

These higher frequency versions of $\omega_+ + \omega_-$ are of particular interest for ICR-ion ejection schemes in cases where the observation of the ion motion must be carried out as quickly as possible, such as the observation of short-lived radioactive ions. The resolution of the system, for a given time of application of the driving field, will be proportional to $m/2$.

The strength of such higher order signals, or the degree to which the orbits motions can be influenced by these higher order multipoles, would be difficult to determine from purely algebraic considerations. However, they could be evaluated by a relaxation calculation of the multipole field strengths and a Runge-Kutta integration through these fields to determine the orbit behavior that results from a variety of starting conditions. As to what may be expected, it can be noted that the electric field strength for an mth order multipole near the center of the trap will vary as the $(m-1)^{th}$ power of the radius. Thus the use of higher azimuthal multipoles will require the application of higher voltages. This in itself could be an advantage since it would increase the applied voltage relative to the noise in the circuit connected to the electrodes of the trap.

In any case, the accuracy of a mass measurement of an ion based on any observation of its $\omega_+ + \omega_-$ will depend on how well this frequency can be related to the q/m of the ion. In the next section we report on a study of effects that can perturb this relationship.

V. THE EFFECTS OF TRAP IMPERFECTIONS

Many of the effects of trap imperfections have been reported in Ref. 12. However, as already mentioned, the work reported in that paper concentrated on the range of parameters of importance in Penning traps for electrons. We will use the formalism of that paper to study the range of parameters of importance in dealing with heavy ions.

A. The effects of electric field imperfections

The practical use of a Penning trap for measuring the mass of an ion will require truncating the infinite hyperboloidal electrodes and introducing devices to inject or produce ions in the trap as well as introducing electric fields into the trap to modify or detect the ion motion. Understanding the effects of the higher order electric field components caused by such deliberate modifications to the pure quadrupole trapping field is therefore an important part of high accuracy measurements using such a trap.

For general electrode geometries, all of the higher order multipoles in (1) will arise. However, again for electrode geometries symmetrical about the $z = 0$ plane, only the even powers of l will contribute. Also, if the electrode geometry provides an azimuthally uniform field for any particular r and z, then only the Legendre polynomials ($m = 0$) will arise. (We will consider the effect of $m \neq 0$ components of the trapping potential in section V-C). For such symmetrical geometries, the precision of which are easily maintained, the potential components arising from modifications of the basic quadrupole geometry of a Penning trap are most conveniently expressed by rewriting the coefficients for these terms as

$$a_l = \frac{V_0}{2z_0^l} C_l \tag{58}$$

where, again, V_0 is the voltage applied to the end electrodes relative to the ring. The coefficients C_l will then be dimensionless representations of the degree of deviation from the pure quadrupole geometry (for which $C_2 = 1, C_{l(\neq 2)} = 0$).

For a given trap geometry with the above symmetries, the coefficients C_l can be evaluated by the relaxation calculation in cylindrical coordinates discussed above. The results for the potential along the z axis can be expressed as the polynomial

$$V(z) = \frac{V_0}{2}\left(C_0 + \frac{C_2}{z_0^2} z^2 + \frac{C_4}{z_0^4} z^4 + \frac{C_6}{z_0^6} z^6 + \dots \right) \tag{59}$$

Fitting a polynomial expansion to the results of the calculation then gives the C_l coefficients.

The method presented in Ref. 12 and based on the formalism introduced in (34) and (36) can be conveniently used to determine the effect of these imperfections on the ion motion frequencies. In this method, the motions are expressed in quantum-mechanical terms and the effects of imperfections evaluated by first-order perturbation. This involves evaluating the energy perturbations of the eigenstates of the three motions due to the deviations from an ideal Penning trap and from these estimating the frequencies for one quantum transitions at various energy levels. Interpreting the energy levels in terms of the classical magnitudes of the oscillations gives the frequencies as functions of these magnitudes.

Considering first the lowest order imperfection in a symmetrical Penning trap, the octupole, the potential imperfection is

$$\Delta V_4 = C_4\left(\frac{V_o}{2}\right)\frac{z^4 - 3z^2 r^2 + \frac{3}{8}r^4}{z_o^4} \tag{60}$$

As given in Ref. 12, the energy perturbation caused by this potential change for a quantum state of the Penning trap motion with quantum numbers n,k and l for the cyclotron, axial and magnetron motion respectively is given by

$$\begin{aligned}\Delta E_{nkl} &= \langle n,k,l \mid q\Delta V \mid n,k,l \rangle \\ &= qC_4\left(\frac{V_o}{2z_o^4}\right)\left(\frac{\hbar}{m}\right)^2 \times\end{aligned}$$

$$\left(\frac{3}{2\omega_z^2}(K^2 + \tfrac{1}{4}) - \frac{6}{\omega_z(\omega_+-\omega_-)}K(N + L) + \frac{3}{2(\omega_+-\omega_-)^2}(N^2 + L^2 + 4NL + \tfrac{1}{2})\right)$$

$$N = n + \tfrac{1}{2}$$

$$K = k + \tfrac{1}{2}$$

$$L = l + \tfrac{1}{2} \tag{61}$$

Taking the increment in this energy shift in going from states n to $n + 1$, k to $k + 1$ and l to $l + 1$, dividing by $\hbar$ and relating the quantum numbers to the classical amplitudes of oscillation through

$$z^2 = \frac{2\hbar}{m\omega_z} K \;;\quad \rho_+^2 = \frac{2\hbar}{m(\omega_+ - \omega_-)} N \text{ and } \rho_-^2 = \frac{2h\hbar}{m(\omega_+ - \omega_-)} L \tag{62}$$

where z is the amplitude of the axial oscillation and ρ_+ and ρ_- are respectively the radii of the cyclotron and magnetron motions, gives

$$\Delta\,\omega_\pm = \pm\frac{3}{4}\frac{C_4}{z_0^2}\frac{\omega_z^2}{(\omega_+ - \omega_-)}\left[\left(\rho_\pm^2 + 2\rho_\mp^2\right) - 2z^2\right)]$$

$$\Delta\,\omega_z = \frac{3}{4}\frac{C_4}{z_0^2}\,\omega_z\left[z^2 - 2(\rho_+^2 + \rho_-^2)\right] \tag{63}$$

and for the important sum frequency

$$\Delta\,(\omega_+ + \omega_-) = \frac{3}{4}\frac{C_4}{z_0^2}\frac{\omega_z^2}{(\omega_+ - \omega_-)}\left(\rho_+^2 - \rho_-^2\right) \tag{64}$$

The next order component which can be of importance in a symmetrical trap is the dodecapole C_6 term. This is expressed in cylindrical coordinates as

$$\Delta V_6 = C_6\left(\frac{V_0}{2}\right)\frac{z^6 - \frac{15}{2}z^4 r^2 + \frac{45}{8}z^4 r^2 - \frac{5}{16}r^6}{z_0^6} \tag{65}$$

Applying a treatment similar to that for the C_4 term gives

$$\begin{aligned}\Delta E_{nkl} = \;& \frac{5}{4}qC_6\left(\frac{V_0}{2z_0^6}\right)\left(\frac{\hbar}{m}\right)^3 \times \\ & \Big\{\ \frac{1}{\omega_z^3}\left(K^3 + \tfrac{5}{4}K\right) - \frac{9}{\omega_z^2(\omega_+ - \omega_-)}K^2(N + L) \\ & + \frac{9}{\omega_z(\omega_+ - \omega_-)^2}K\left(N^2 + L^2 + 4NL + \tfrac{1}{2}\right) \\ & - \frac{1}{(\omega_+ - \omega_-)^3}\left[N^3 + L^3 + 9NL^2 + \tfrac{9}{2}(N + L\right]\ \Big\}\end{aligned} \tag{66}$$

and

$$\Delta \omega_{\pm} = \pm \frac{15}{16} \frac{C_6}{z_0^4} \frac{\omega_z^2}{(\omega_+ - \omega_-)} \left[-3z^4 + 6z^2(\rho_{\pm}^2 + 2\rho_{\mp}^2) - (\rho_{\pm}^4 + 3\rho_{\mp}^4 + 6\rho_+^2\rho_-^2) \right]$$

$$\Delta \omega_z = \frac{15}{16} \frac{C_6}{z_0^4} \omega_z \left[z^4 - 6z^2(\rho_-^2 - \rho_+^2) + (\rho_+^4 - \rho_-^4) \right]$$

$$\Delta (\omega_+ + \omega_-) = \frac{15}{8} \frac{C_6}{z_0^4} \frac{\omega_z^2}{(\omega_+ - \omega_-)} \left[3z^2(\rho_-^2 - \rho_+^2) + (\rho_+^4 - \rho_-^4) \right] \qquad (67)$$

It is seen that the dodecapole component introduces a dependence of the sum frequency on the amplitude of the z motion. Applying the above analysis to the Penning trap in the ISOLDE system, which has $r_0 = \sqrt{2}z_0 = 8$ mm and cylindrical holes of 2 mm diameter through the centers of the end electrodes to allow entry and exit of ions gives the results

$$C_0 = -\ 1.00; \quad C_2 = +0.96; \quad C_4 = +0.23; \quad C_6 = -\ 0.26 \qquad (68)$$

The ISOLDE Penning trap is operated in a magnetic field of 6 T with a trapping potential V_0 of 10 V. The frequency shift for a representative z amplitude of 2 mm and cyclotron and magnetron radii of 0.1 mm and 1.0 mm respectively is about 45 Hz from the octupole imperfections and –43 Hz from the dodecapole trap imperfections.

Thus, even though it is of higher order, the dodecapole component can have about the same effect on the sum frequency as the octupole component. This is because of the larger coefficients in (67) compared to (64) and the z amplitude being larger than the cyclotron and magnetron radii. If there is a spread of axial oscillation amplitudes of the ions in the trap there will then be a significant spread in the sum frequency of the cyclotron and magnetron motions, due primarily to the dodecapole imperfection. The effect of this imperfection for various ion motions in the ISOLDE trap is shown in Fig. 5.

In this figure, the results are also given for a numerical integration of the trajectories using a fourth-order Runge-Kutta routine and a Fourier analysis of the time behavior of the x coordinates. The validity of the first order perturbation calculation is demonstrated by the fit of the calculated points to the graph of (67), the deviations being easily attributable to the calculational errors in the numerical integrations.

Accurate mass measurement in this Penning trap would therefore require compensating both the octupole and the dodecapole components of the electric field in the trap. For motions extending to amplitudes and radii of about 10% of z_0 and accuracies of the order of 1 part in 10^7, this will require reducing these components to about 1% of their uncorrected value. The octupole component can be corrected by the usual technique of introducing extra ring electrodes in the gap between the main ring and the end electrodes[12]. However, a correction of the dodecapole imperfection requires another set of electrodes which are most effectively placed at the holes, i.e at the principle source of that imperfection.

It can be noted that the contribution of each of these higher order field components gives a deviation in the sum frequency which has the dependence

$$\frac{\Delta\,(\nu_+ + \nu_-)}{\nu_c} \sim \text{const.} \times \frac{\nu_z^2}{\nu_c^2} \tag{69}$$

Representative values for the operating parameters of electron traps and proton traps are given in Tables I and II in Ref. 12. They show that the ratio of axial to cyclotron frequency for electron traps is about 300 times larger than this same ratio for a proton trap. The effects of the higher multipole components in the trap operation are therefore much more important for heavy ions then for the electron of Geonium, especially since the electron will have its motion very effectively cooled to very small orbit radii by synchrotron radiation. A trap designed for use in the measurement of the masses of heavy ions should therefore have correction electrodes for at least the octupole and dodecapole imperfections.

This analysis could be extended to higher order components. However, because the effects are proportional to the power m-2 of the ratio of the amplitudes of the motions to the trap dimension z_0, the effect of these higher order components for ions confined to small distances from the trap center should be negligible compared to those of the octupole and dodecapole.

B. The effects of magnetic field inhomogeneity

In a practical Penning trap, a magnetic field inhomogeneity could arise from two sources; the finite extent of the solenoidal windings creating the magnetic field and distortion of this field by the magnetic susceptibility of the material forming the electrodes of the trap. It both cases, it can be assumed that the imperfection can be made symmetrical about z = 0. The lowest order component of the magnetic field inhomogeneity will then be the quadrupole expressed as

$$B_z = B_0\,(\,1 + \beta_2\left(z^2 - \frac{r^2}{2}\right)\,) \tag{70}$$

In Ref. 12 only the effect of the magnetic inhomogeneity on the frequency of the axial motion is presented. This is because usually the cyclotron frequency is experimentally inaccessible for electron motion because it is very high. Applying the techniques used in Ref. 12 to the cyclotron motion gives

$$\Delta\,\omega_c = \beta_2\omega_c\left[\,z^2 - \frac{\rho_+^2}{2}\left(1 - \frac{\omega_c}{\omega_+ - \omega_-}\right) - \frac{\rho_-^2}{2}\left(1 + \frac{\omega_c}{\omega_+ - \omega_-}\right)\right] \tag{71}$$

which, in the approximation $\omega_c \approx \omega_+ - \omega_-$, gives

$$\Delta\,\omega_c = \beta_2\omega_c \left[z^2 - \rho_-^2 \right] \tag{72}$$

With modern high-homogeneity superconducting solenoids, it is expected that the major contribution to the inhomogeneity will be the electrodes of the trap itself. Calculation of the inhomogeneity due to the electrodes of the trap used at ISOLDE gives

$$\beta_2 \;=\; -1.7\times 10^{-7} \tag{73}$$

which, for representative amplitudes of 1 mm for ρ_- motion and 2 mm for the z amplitude gives;

$$\frac{\Delta\,\omega_c}{\omega_c} \;=\; -6\times 10^{-7} \tag{74}$$

C. The effects of misalignments of the electrodes and the magnetic field

It is shown in Ref. 12 that the effects of minor asymmetries in the electrodes of a Penning trap can be expressed in a "principal-axis" coordinate system as small $m > 1$ components added to the $l = 2$, $m = 0$ component forming the basic trapping field. The lowest order of these perturbations is, of course, the azimuthal quadrupole component which can be expressed in terms of an ellipticity parameter ε;

$$\phi = \frac{1}{2}\, m\omega_z^2 \left[z^2 - \frac{1}{2}(x^2+y^2) - \frac{1}{2}\varepsilon\,(x^2-y^2) \right] \tag{75}$$

Such an ellipticity can arise from an asymmetry in the electrodes such as a slit in the ring electrode to make a dipole configuration, or a misalignment of the symmetry plane of the ring electrode with the principle axis.

A misalignment of the magnetic field with the principle axis of the system can be expressed as components of the magnetic field in terms of the angle θ between the magnetic field at the trap center and the principle axis and the angle φ that the x axis makes with the plane containing the principle axis and the magnetic field vector;

$$B_x = B\ \sin\theta\ \cos\varphi,\ B_y = B\ \sin\theta\ \sin\varphi\ ,\ B_z = B\ \cos\theta \tag{76}$$

In Ref. 12 it is shown that the effects of this misalignment and the ellipticity is to perturb the frequencies from the values for an aligned and symmetric trap, ω_+, ω_- and ω_z, to the values $\bar{\omega}_+$, $\bar{\omega}_-$ and $\bar{\omega}_z$ related through the equations

$$\begin{aligned}
\bar{\omega}_+^2\bar{\omega}_-^2\bar{\omega}_z^2 &= \tfrac{1}{4}\omega_z^6\,(1 - \varepsilon^2) \\
\bar{\omega}_+^2\bar{\omega}_z^2 + \bar{\omega}_+^2\bar{\omega}_-^2 + \bar{\omega}_-^2\bar{\omega}_z^2 &= \omega_+^2\omega_-^2\left(1 - \tfrac{3}{2}\sin^2\theta - \tfrac{\varepsilon}{2}\sin^2\theta\cos 2\varphi\right) \\
&\quad - \tfrac{3}{4}\omega_z^4\,(1 + \tfrac{\varepsilon^2}{3}) \\
\bar{\omega}_+^2 + \bar{\omega}_-^2 + \bar{\omega}_z^2 &= \omega_c^2
\end{aligned} \tag{77}$$

For a given set of trap parameters, these equations show that the deviation of the sum frequency $\bar{\omega}_+ + \bar{\omega}_-$ from ω_c will depend on the ratio of ω_z to ω_c. This ratio, in turn, will depend on the mass of the ion. We estimate that the largest possible values for θ and ε for the trap at ISOLDE are $\theta = 0.01$ and $\varepsilon = 0.01$. Solving (79) for these parameter values (the φ dependence is insignificant) gives the dependencies of the deviation on the ion mass shown in Fig. 6.

The effect of these asymmetries is thus to introduce a fractional deviation of $\bar{\omega}$ $)_+ + \bar{\omega}_-$ ($\equiv \bar{\omega}_c$) from ω_c which is linearly dependent on the ion mass. This is important in the calibration of the trap as a mass spectrometer. Any such calibration must be carried out by a comparison of the observed cyclotron frequency for an ion of unknown mass with that for an ion of known mass. Expressing the correction $\Delta\omega_c = \bar{\omega}_c - \omega_c$ by a coefficient γ defined by

$$\gamma = \frac{\mathrm{d}}{\mathrm{d}A}\left(\frac{\Delta\omega_c}{\omega_c}\right) \tag{78}$$

gives the calibration correction factor R defined by the relation

$$m^a = m^b \left(\frac{\bar{\omega}_c^b}{\bar{\omega}_c^a}\right)(1 + \mathrm{R}) \tag{79}$$

as

$$R = \gamma\,(A^a - A^b) \tag{80}$$

where $m^a = m^b$ are the unknown and the calibration masses respectively and A^a - A^b are those masses in atomic mass units. For the two cases shown in Fig. 6 the values of γ are about 3×10^{-9} and 9×10^{-9} showing that, even for these extreme cases, the calibration error will be less than 1 part in 10^7 for differences of 10 atomic units between the calibration and the unknown masses.

D. Space charge effects

The original paper on ICR cells[8] stated that space charge electric fields present a "different but related effect" to that of the applied trapping voltage. It is different in that it is not fixed by the geometry and externally applied fields of the trap but depends on the distribution of the various ion components in the ion cloud in the trap, the properties of which are very difficult to determine or to control. It is related in that the space charge effect does also depend on the field parameters of the trap.

The space charge effect is most easily understood for a cloud of ions of a single ion species. It was originally pointed out by Wineland and Dehmelt[14] that the space charge of such a cloud of ions does not influence the center-of-mass motion of the cloud. Thus, as pointed out by Jeffries et al[30], if the electric field used to excite or detect the ion motion interacts only through the center-of-mass of the cloud, there will be no shift of the observed cyclotron or magnetron frequencies. This was confirmed in the work of Wineland et al[7], as reported in ref. 11, where observed magnetron frequencies were the same as single ion values to within experimental accuracies (≈ 0.5%) but the magnetron frequencies of individual ions, determined by Doppler shift measurements on optical transitions, were up to three times larger.

Thus space charge effects of a single ion species in a perfect Penning trap will not directly cause a shift in the observed cyclotron and magnetron frequencies. However, if the space charge forces a significant fraction of the ions out of the central region of the trap into the region were field imperfections can cause frequency shifts, then there will be, indirectly, a frequency shift which is space charge dependent. This is probably the cause of the shift in $\omega_+ + \omega_-$ as a function of proton number seen in the experimental results published in ref. 20.

Thus a reduction of space charge effects requires either a reduction in the number of ions or a reduction in the trap imperfections discussed above. The number of ions that can be tolerated will depend on the volume throughout which the field imperfections can be made to have negligible effect and so, in general, larger traps will be useful for greater numbers of ions. Alternately, larger traps can be used for greater accuracy with the same number of ions. The number of ions that can be used in a particular trap is probably best determined by experiment. As a representative figure, be useful for greater numbers of ions. Alternately, larger traps can be used for greater accuracy with the same number of ions. The number of ions that can be used in a particular trap is probably best determined by experiment. As a representative figure, ref. 7 reports an uncertainty of 0.34 ppm when working with 20 $^9Be^+$ ions in a roughly spherical cloud of diameter 0.1 mm in a Penning trap with $z_0 \approx 2.5$ mm, operated in a field of 1.13 T at $V_0 = 1$ V.

Space charge effects between ions of the same species are not all deleterious for ICR in a Penning trap. The Coulomb interactions between the individual ions serve to thermalize the ion motion about the center-of-mass motion and this can reduce the spread in the time-of-flight signal in the ion ejection scheme of ICR detection. Using the approach of Spitzer[31] it can be estimated[32] that, for the ISOLDE Penning trap, thermalization times of less than a second will occur for 100 ions of mass A = 100 in a density of 10^6 cm^{-3}.

The space charge effect with more than one ion species in the trap is much more severe. Here the center-of-mass motions of the two species can interact to cause very large shifts of the cyclotron frequencies. For example, in ref. 11 it is reported that a single $^9BeH^+$ ion broadens the cyclotron resonance of $^9Be^+$ by more than 100 ppm. Space charge effects with multiple ion species in the trap have been thoroughly analyzed in ref. 30 with experimental results using FT-ICR in ref. 5. In essence, the cyclotron frequencies of an ion species will be quite significantly effected by the presence of the other ion species and accurate mass measurements can only be carried out by having at least two calibration ions in the trap with masses near that of the unknown.

High accuracy absolute mass measurements by ICR in a Penning trap therefore seems to require that there be no contaminating ions in the trap. This was the approach taken in the work of ref. 20 and in ref. 11 where contaminating ions were driven from the trap by strong dipole excitation of the cyclotron motion before any observations of the cyclotron frequencies of the desired ions.

E. Effects of Trap Imperfections On Resolution

Except for misalignments, the imperfections of a Penning trap used for TOF-ICR will introduce a spread in the TOF of the ejected ions. The extent of this spread will depend on the range of their initial cyclotron and magnetron radii and their initial axial oscillation amplitudes and upon the electric field of the space charge of the ion cloud. In a scan through the magnetron-cyclotron resonance this spread in TOF will convolve with the resonance, causing the observed resonance in general to be broader than that which would be seen for the pure trap as deduced from fig. 4.

The initial magnetron radii can be kept under control by a restricting aperture placed in front of the trap and the initial cyclotron radii can be controlled by focussing the ion trajectories onto the magnetic field lines leading through this aperture at some point in the magnetic field of the solenoid where the subsequent ion motion to the trap center will be adiabatic in orbital magnetic moment. For the ISOLDE apparatus, the focussing is done at 20 cm from the trap center where the magnetic field is about 4.3 T and the restricting diaphragm at 27.5 cm from the trap center where the magnetic field is about 2.5 T.

The axial ion motion is more difficult to restrict at injection. However, the extent of the axial motion after resonance can be deduced by using a sequence of short extraction pulses (pips) superimposed on a slowly rising ramp, as used in the original system of ref. 20 and as used in the ISOLDE apparatus. Selecting the TOF observations on the basis of the pips to which they are related, allows some control over the axial motion in the TOF observations.

The effects of the space charge of contaminant ions can only be eliminated by eliminating the offending ions themselves. An example is shown in Fig. 7 where the effect of ^{87}Rb on the resonance of ^{85}Rb can be seen in the scan on the left. Such an effect can only be avoided by not having such offending ions in the initial injection or by removing them from the trap after injection and before magnetron-cyclotron resonance is applied. The resonance shown on the right was obtained after the major part of the contaminant ^{87}Rb was removed by directly exciting its cyclotron resonance using a dipole configuration for the ring electrode circuit.

The best results that have been obtained with the ISOLDE apparatus are shown in Fig. 8. This was obtained with initial magnetron radii centered on about 1 mm and with an estimated spread of 0.3 mm and with a similar spread in cyclotron radii. The spread in axial amplitude is estimated to be about 1 mm. It is seen that the observed resonance an estimated spread of 0.3 mm and with a similar spread in cyclotron radii. The spread in axial amplitude is estimated to be about 1 mm. It is seen that the observed resonance in this particular case is a narrow one superimposed on a broader one, the broader one probably being due to inadequate selection of the axial motion amplitudes.

The half-width of the narrow resonance of Fig. 8 is about 0.3 Hz, corresponding to a resolving power of over 2 000 000. This is only about 10% less than the Fourier-Transform limit. for a 3.6 s observation of a 685 kHz signal and so the resolution could be improved even further by lengthening the time of application of the rf field. However, the very low rf voltages required for such operation, and the longer cycle times, make such a resolution generally impractical. Furthermore, as pointed out in the introduction to this paper, high resolution does not automatically lead to high accuracy. For high accuracy in TOF-ICR mass spectrometry, the number achieved for the magnetron-cyclotron resonance must be related to the mass of the ions being observed.

VI. PRECISION AND ACCURACY OF TOF-ICR

Any accurate measurement of an unknown mass using TOF-ICR will involve a measurement of a frequency associated with the motion of the unknown ion in the trap and a similar measurement of a frequency for a known calibration mass. It is useful to consider the overall accuracy of the measurement as resulting from two factors, the statistical precision to which the frequency can be determined and the systematic errors limiting the accuracy with which the mass can be determined from this frequency.

The precision in TOF-ICR mass spectroscopy will be related to the accuracy which which the dip of the time of flight can be located on the frequency scan. This will be most directly related to the resolution that can be obtained, as discussed in the preceding section, but it can also depend on the statistical variation of the observed TOF numbers for a given scan. In general it is expected that, from the sort of scans that have been obtained with the ISOLDE apparatus, the precision of the resonance frequency from the TOF scan can be better than 0.1 ppm.

The accuracy of a mass measurement will depend on how well the ratio of these precise numbers for an unknown and a calibration ion can be related to their mass ratio. From (72) the deviation of the cyclotron plus magnetron frequency due to the magnetic field inhomogeneity is proportional to the unperturbed cyclotron frequency itself, provided the magnetron radii and the axial oscillation amplitudes are the same for the unknown and the calibration ions. Furthermore, this deviation is rather small. Thus, provided the geometry of the trajectories for the unknown and the calibration masses can be made reasonably similar, the mass ratio will be unaffected by the deviation caused by such an inhomogeneity.

The uncertainty introduced by asymmetries in the trap have already been discussed in section V-C. There it is shown that the proportionality constant between the cyclotron-magnetron sum frequency and the ion mass will depend on these asymmetries. However, the typical effect will be less than 0.1 ppm for differences up to 10 atomic mass units between the unknown and the calibration masses and presumably even this small error can be calibrated by using a variety of calibration masses.

The most serious trap imperfection in mass spectroscopy by ICR in a Penning trap is therefore that of the electric fields experienced by the ions. As already shown, the effect of the electric field of the space charge of contaminating ions can be removed by removing those ions. This leaves the effect of the imperfections of the trapping field as the most significant.

by removing those ions. This leaves the effect of the imperfections of the trapping field as the most significant.

The dependence of the cyclotron-magnetron sum frequency on the octapole and dodecapole components of the trapping field have been presented in (63) and (67). It is seen that the deviations from the unperturbed cyclotron frequency depends not only on the axial oscillation amplitude but also on the cyclotron and magnetron radii. Thus as the magnetron radii shrink and the cyclotron radii grow during a magnetron-cyclotron "resonance", the deviation of the magnetron-cyclotron sum frequency from the unperturbed cyclotron frequency changes. An applied field of frequency equal to the unperturbed cyclotron frequency will only be at resonance with the magnetron-cyclotron sum frequency when the cyclotron radius exactly equals the magnetron radius. It will therefore generally be off-resonance and more applied field then that indicated by (56) will be necessary to complete the full transform in a given time. Also, it can be expected that the energy absorption from the applied field for a given application interval will not be a symmetrical function of the frequency of the applied field.

However, there will be a field strength at which an initial magnetron motion will be completely converted into cyclotron motion in a given time interval when the applied field is in resonance with the cyclotron-magnetron sum frequency. If the applied field is of constant amplitude, then the ions will spend the same amount of time with magnetron radius greater than cyclotron radius as with the reverse. From the antisymmetry of (63) and (67) in cyclotron and magnetron radii, it can be seen that the average deviation of the cyclotron-magnetron sum frequency from the unperturbed cyclotron frequency will be zero. This effect can be seen in the results of a computer simulation of the ion motion in a trap with the imperfections calculated to be in the trap of the ISOLDE apparatus. This is shown in Fig. 9.

Results of scanning the magnetron-cyclotron resonance at various applied field strengths in the ISOLDE apparatus is shown in Fig. 10. It is seen that the shift in the observed resonance frequency changes from being positive when the field strength is insufficient to give the maximum time of flight effect to being negative when it is too great. The true unperturbed cyclotron frequency is presumably near that of the resonance when the time of flight effect is the greatest.

The accuracy of the mass determination will depend on how well this deviation of the frequency of the observed resonance from the unperturbed cyclotron frequency can be maintained for the observation of the unknown mass and the calibration mass. From the present results with the ISOLDE apparatus, it appears that this can be maintained to well within 0.5 ppm and it is thought that with planned improvements to the system and more experience with calibration masses so as to identify the sources of systematic errors, absolute accuracies of 0.1 ppm should be possible.

VII. THE COOLING OF IONS IN A PENNING TRAP

From the above it is clear that accuracy of mass measurements using ICR in a Penning trap is considerably enhanced by confining ion motion to within well defined limits near the trap center. For ions that are created or injected into the trap with phase space larger than desired, it would be advantageous to cool their motions so that more of them could be injected into the useful phase space volume of the trap.

Cooling of ion motion in a Penning trap is complicated by the negative total energy of the magnetron motion. Simply removing energy from the three degrees of freedom causes the ions to migrate outward radially from the trap center. Wineland et al[33] have studied this problem in connection with laser sideband cooling of ion motion in a Penning trap and have shown that the magnetron kinetic energy can be removed, causing the ion to move toward the center of the trap, by using two laser beams directed perpendicular to the trap axis and at frequencies $\omega_0 - \omega_+$ and $\omega_0 + \omega_-$ where ω_0 is the ionic optical transition frequency used for the sideband cooling.

The analysis of ion motion under an applied rf field presented above suggests another method of cooling. It has been shown that applying an azimuthal quadrupole rf field at $\omega_+ + \omega_-$ will convert magnetron motion into cyclotron motion. A small amount of buffer gas introduced into the trap will cool the axial and the cyclotron motions. (Cooling of ion motion in RFQ traps by helium as a buffer gas is a common technique.[34]) By adjusting the strength of the applied rf quadrupole field so that the rate of transformation of the magnetron to cyclotron motion is commensurate with the cooling rate of the cyclotron motion, the kinetic energy in all three degrees of freedom would be removed and the ions still moved toward the center of the trap.

The application of such a scheme directly to a Penning trap for mass measurements would considerably complicate its operation. Not only would the buffer gas have to be introduced; it would have to be removed before accurate cyclotron resonance measurements could be made. Also, for observation of the $\omega_+ + \omega_-$ frequency, a magnetron motion would have to be reintroduced by a suitable dipole excitation. In a system where the ions are produced and prepared outside and injected into the measuring trap, as in the mass measuring system installed at ISOLDE, it would be desirable to condense the phase space volume of the ions by cooling in the external excitation. In a system where the ions are produced and prepared outside and injected into the measuring trap, as in the mass measuring system installed at ISOLDE, it would be desirable to condense the phase space volume of the ions by cooling in the external collection trap. The transport system could then place the ions in the measuring Penning trap with the desired initial magnetron motion. With care, this transport system could be designed to preserve the small phase space volume about this central motion.

Such a scheme is now being tested with the ISOLDE system and, if successful, will be used in future measurements with the system.

VIII. SUMMARY AND CONCLUSIONS

The application of the above analysis to the mass measurement system installed at ISOLDE has shown that it is capable of resolutions of over 2 000 000 for mass number A ~ 100 and accuracies of better than 0.5 ppm, and that the major sources of inaccuracy in that system are the octupole ($l = 4$) and the dodecapole ($l = 6$) components in the trapping electric field with some additional uncertainty caused by magnetic field inhomogeneity due to diamagnetism of the copper electrodes of the trap. A detailed analysis of the measurements made with this system is now being undertaken and the results will be published when completed. Meanwhile, enough has been learned to establish the features required in a high-accuracy system designed for resolutions of greater than 1 ppm and accuracies of 0.1 ppm. These are:

1. The Penning trap must be as large as possible and cause as little distortion of the magnetic field as possible.

2. The ring electrode must be divided into quadrants to provide the required azimuthal quadrupole electric field for detection of the $\omega_+ + \omega_-$ resonance. The circuit connected to these quadrants should be capable of exciting a dipole field for possible removal of contaminating ions.

3. The geometrical symmetry of the electrode configuration should be preserved to better than 1% of z_0 or about 0.1-mm for a practical design for the ISOLDE system.

4. There must be correction electrodes for both the octupole and dodecapole components of the trapping electric field caused by the holes for ion entrance and extraction.

5. It must be possible to accurately align the system for the injection of the ions into the Penning trap with a precisely controlled phase space volume. The axial dimensions of this volume are controlled by the amplitude and timing of the retardation voltage. The radial motion is controlled by the alignment of the ion path with the magnetic field lines of the solenoid.

A new Penning trap and injection system has been designed to satisfy these demands. A cross-sectional view of the trap is shown in Fig. 11.

REFERENCES

[1]Proc. of the 11^{th} Int. Mass Spectrom. Conf., Bordeaux, 1988, "Advances in Mass Spectrometry", Vol. 11a and 11b ed. by P. Longevialle Heyden & Son Ltd., London, 1989.

[2]K.P. Wanczek, Proc. 7^{th} Intn'l Dynamic Mass Spectrometry Symposium, Salford, 1989, (to be published).

[3]E. Koets, J. Phys. E., **14,** 1229 (1981).

[4]E.B. Ledford, Jr., S.G. Ghaderi, R.L. White, R.B. Soencer, P.S. Kulkarni, C.L. Wilkins and M.L. Gross, Anal. Chem., **52,** 463 (1980).

[5]T.J. Francl, M.G. Sherman, R.L. Hunter, M.J. Locke, W.D. Bowers and R.T. McIver, Jr., Int. J. Mass Spectrom. Ion Proc., **54**, 189 (1983).

[6]R.S. Van Dyke, Jr., P.B. Schwinberg and H.G. Dehmelt, in Atomic Physics 9 (1984), edited by R.S. Dyke, Jr. and E.N. Fortson (World Scientific, Singapore).

[7]D.J. Wineland, J.J. Bollinger and Wayne M. Itano, Phys. Rev. Lett. **50**, 628 (1983).

[8]H. Sommer, H.A. Thomas and J.A. Hipple, Phys. Rev. **82**, 697 (1951).

[9]J.A. Hipple, H. Sommer and H.A. Thomas, Phys. Rev. **76**, 1877 (1949).

[10]J. Byrne and P.S. Farago, Proc. Phys. Soc. London, **86** 801 (1965)

[11]D.J. Wineland, Wayne M. Itano, J.C. Bergquist, J.J. Bollinger and J.D. Prestage, Atom. Phys. **9**, (1985).

[12]L.S. Brown and G. Gabrielse, Rev. Mod. Phys. **58**, 233 (1986).

[13]M.B. Comisarow, J. Chem. Phys. **69** 4097(1978).

[14]D.J. Wineland and H.G. Dehmelt, Jour. Appl. Phys. **46**, 919 (1975).

[15]L. Schweikhard, M. Blundschling, R. Jertz and H.-J. Kluge, Rev. Sci. Instrum. **60** (1989) 2631.

[16]W.H. Press, B.P. Flannery, S.A Teulolsky and W.T. Vetterling, "Numerical Recipes", Cambridge University Press, Cambridge, 652(1986).

[17]D.L. Rempel, E.B. Ledford, Jr., S.K. Huang and M.L. Gloss, Anal. Chem. **59** (1987), 2527.

[18]L. Schweikhard, M. Lindinger, H.-J. Kluge. (Submitted for publication to Rev. Sci. Instrum.)

[19]lL. Schweikhard, M. Lindinger and H.-J. Kluge, Int. J. Mass Spectrom. Ion Phys., (submitted for publication).

[20]G. Gräff, H. Kalinowsky, and J. Traut, Z. Phys. **A 297**,35 (1980).

[21]F. Bloch, Physica 19, 821(1953).

[22]P. Dabkiewicz, H. Kalinowsky, F. Kern, H.-J. Kluge, L. Schweikhard, H. Schnatz, H. Stürmer and R.B. Moore, Proceedings of Mont-Gabriel Workshop, June 1984. TRIUMF Publication TRI-84-l.

[23]P. Dabkiewicz, H. Kalinowski, F. Kern, H.-J. Kluge, L. Schweikhard, H. Schnatz, H. Stürmer and R.B. Moore, Proc. of 7th Int. Conf. on "Atomic Masses and Fundamental Constants",(AMCO-7), Darmstadt-Seeheim,1984, ed. by O. Klepper, p.684.

[24]H. Schnatz, G. Bollen, P. Dabkiewicz, P. Egelhof, F. Kern, H. Kalinowsky, L. Schweikhard, H. Stolzenberg, H.-J. Kluge and the ISOLDE Collaboration, Nucl. Instr. and Meth. **A251**, 17 (1986).

[25]G. Bollen, P. Dabkiewicz, P. Egelhof, T. Hilberath, H. Kalinowsky, F. Kern, H. Schnatz, L. Schweikhard, H. Stolzenberg, R.B. Moore, H.-J. Kluge, G. Temmer, G. Ulm and the ISOLDE Collaboration, Hyperfine Interact. **38**, 793 (1987).

[26]H.-J. Kluge, Physica Scripta, **T-22**, 85 (1988).

[27]F. Kern, P. Egelhof, T. Hilberath, H. Kalinowsky, H.-J. Kluge, K. Kunz, L. Schweikhard, H. Stolzenberg, R.B. Moore, G. Audi, G. Bollen and The ISOLDE Collaboration, Proceedings of the 5^{th} Int. Conf. on Nuclei far from Stability, Rosseau Lake, AIP Conf, Proc. **164**, p. 22, Amer. Inst. of Phys, New York (1988).

[28]G. Audi, G. Bollen, P. Egelhof, H.-J. Kluge, F. Kern, K. Kunz, R.B. Moore, L. Schweikhard, H. Stolzenberg and The ISOLDE Collaboration, Proceedings of the 11^{th} Int. Mass Spectrom. Conf., Bordeaux, 1988 (see ref. 1).

[29]G. Gräff, "Ion Cyclotron Resonance Spectrometry II", H. Hartmann and K.-P. Wanczek editors, Lecture Notes in Chemistry Series of Springer Verlag, Proc. of 2nd Int. Symp. on Ion Cyc. Res. Spectrom., (1982), p. 318.

[30]J.B. Jeffries, S.E. Barlow and G.H. Dunn, Int. J. Mass Spectrom. Ion Proc., **54**, 169 (1983).

[31]L. Spitzer Jr., "Physics of Fully Ionized Gases", Interscience, New York (1956).

[32]G. Bollen, PhD. Thesis, Mainz (1989) (In German - Unpublished).

[33]D.J. Wineland, Wayne M. Itano, J.C. Bergquist, and R.G. Hulet, Phys. Rev. A, **36**, 2220 (1987).

[34]A. Alili, J. André and F. Vedel, Physica Scripta, **T22**, 325 (1988).

FIGURE CAPTIONS

Fig. 1 A simple system of two electrodes in which the energy absorbed by an ion motion is replaced by a current from a potential supply.

Fig. 2 The response of a system with a natural oscillation frequency when driven for a time T at a frequency which deviates from the natural frequency. To have the same graph applicable to all driving times, the frequency deviation is expressed in units of $1/T$.

Fig. 3. The result of the numerical integration of the equations of motion for a particle in a Penning trap with an applied azimuthal quadrupole electric field of frequency equal to the sum of the cyclotron and magnetron frequencies. The initial motion was chosen to be completely magnetron and the quadrupole field strength was chosen to cause a transition to completely cyclotron motion in about 60 cyclotron orbits. Frame 1 shows the first 32 orbits whereupon the cyclotron and the magnetron radius have become equal. Here, as in frame 4, the trace for an undisturbed magnetron orbit is shown for reference. Frame 2 shows the orbits leading to complete cyclotron motion while 3 and 4 show the progression back to complete magnetron motion.

Fig. 4. The orbital energy at the end of application of various quadrupole field strengths for a specific time. The quadrupole field strength which would completely transform the initial magnetron motion into cyclotron motion in this time when applied in resonance to $\omega_+ + \omega_-$ is denoted be a_{max}. When this strength is twice this value, it is seen that the cyclotron energy has returned to zero at the resonant frequency.

Fig. 5. The effect of the dodecapole term (65) on the frequencies of the motion of an ion in a Penning trap with $z_0 = 6$-mm operated in a magnetic field of 6-T with a trapping potential V_0 of 10-V. The curves show the results of calculations using (67). The results of a numerical integration of the trajectories using a fourth-order Runge-Kutta routine and a Fourier analysis of the time behavior of the x coordinates are shown as points. The agreement, which is within the accuracy of the integration, shows the validity of the first order perturbation approach.

Fig. 6 The dependence of the deviation of $\bar{\omega}_+ + \bar{\omega}_-$ from ω_c on ion mass number for representative magnetic field misalignment and trap eccentricity parameters.

Fig. 7 Resonances showing the effect of ion contamination in the measuring trap. On the left are shown the broadened resonances obtained with rubidium ions of the natural abundance ratios of ^{85,87}Rb. For the figure on the right, the ^{85}Rb ions were excited to a larger cyclotron radius by dipole excitation before application of the rf field at ω_c. As a result, there is no ^{87}Rb signal and the ^{85}Rb signal becomes much narrower. The frequency scales are broken in the middle of each figure so as to incorporate the data for both isotopes.

Fig. 8 A recent resonance obtained on ^{133}Cs ions at $\omega_+ + \omega_-$ with cooling of the ions in the collection trap before delivery to the measuring trap. The resonance frequency was 685075.6-Hz with a FWHM of 0.3 Hz. The duration of the rf field was 3.6 s. The FWHM is calculated for a gaussian fitted to the central peak. The broader background under this peak is probably due to ions which have not been cooled to the same degree as those contributing to the peak.

Fig. 9. The solid curve shows orbital energy at the end of application of an rf quadrupole field strength for a specific time of a strength 1.4 times that which would have completely converted an initial magnetron motion into a cyclotron motion with the octupole and the dodecapole components determined to be in the ISOLDE measuring Penning trap. The dashed curve shows the maximum energy achieved during the conversion cycle. It is seen that this peaks at zero frequency shift.

Fig. 10 Variation, with applied field strength, of the TOF (a) and of the resonance frequency (b) at resonance on $\omega_+ + \omega_-$ for ^{133}Cs ions in the Penning trap. The duration of application of the rf field was 900 ms in all cases. The zero for the frequency scale in (b) is at the frequency which gave the maximum TOF effect, in this case 685100.36 Hz. The shaded curves are from estimates of the time of flight effect which would have a maximum at the same position as the data as shown in (a) and based on numerical integration of the equations of motion including the estimated C_4 and C_6 electric field components of the trap.

Fig. 11 Cross-sectional view of the new Penning trap to be installed in the ISOLDE mass measuring system.

Figure 1.

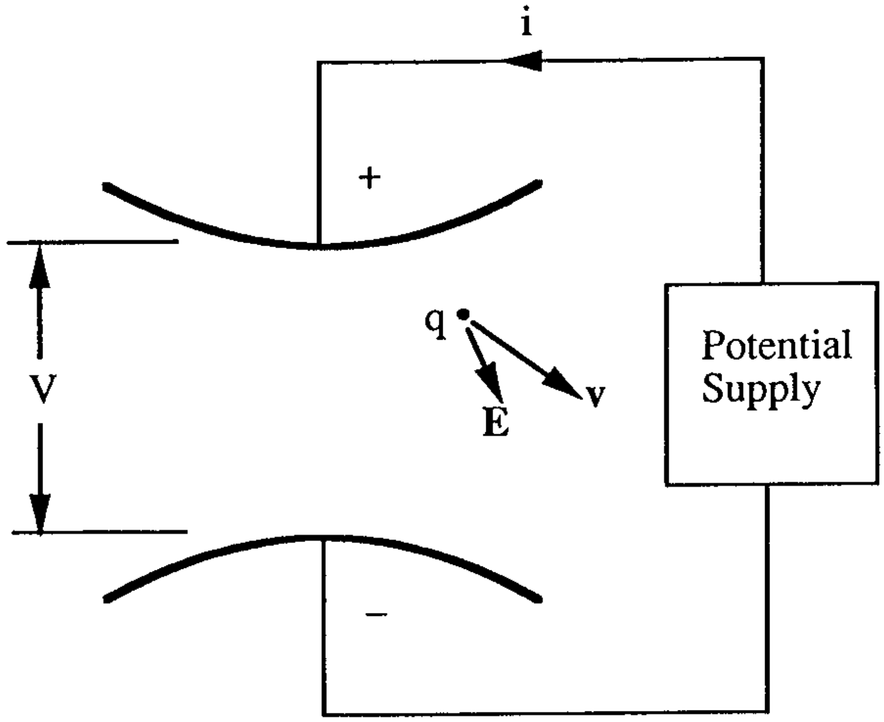

Figure 2.

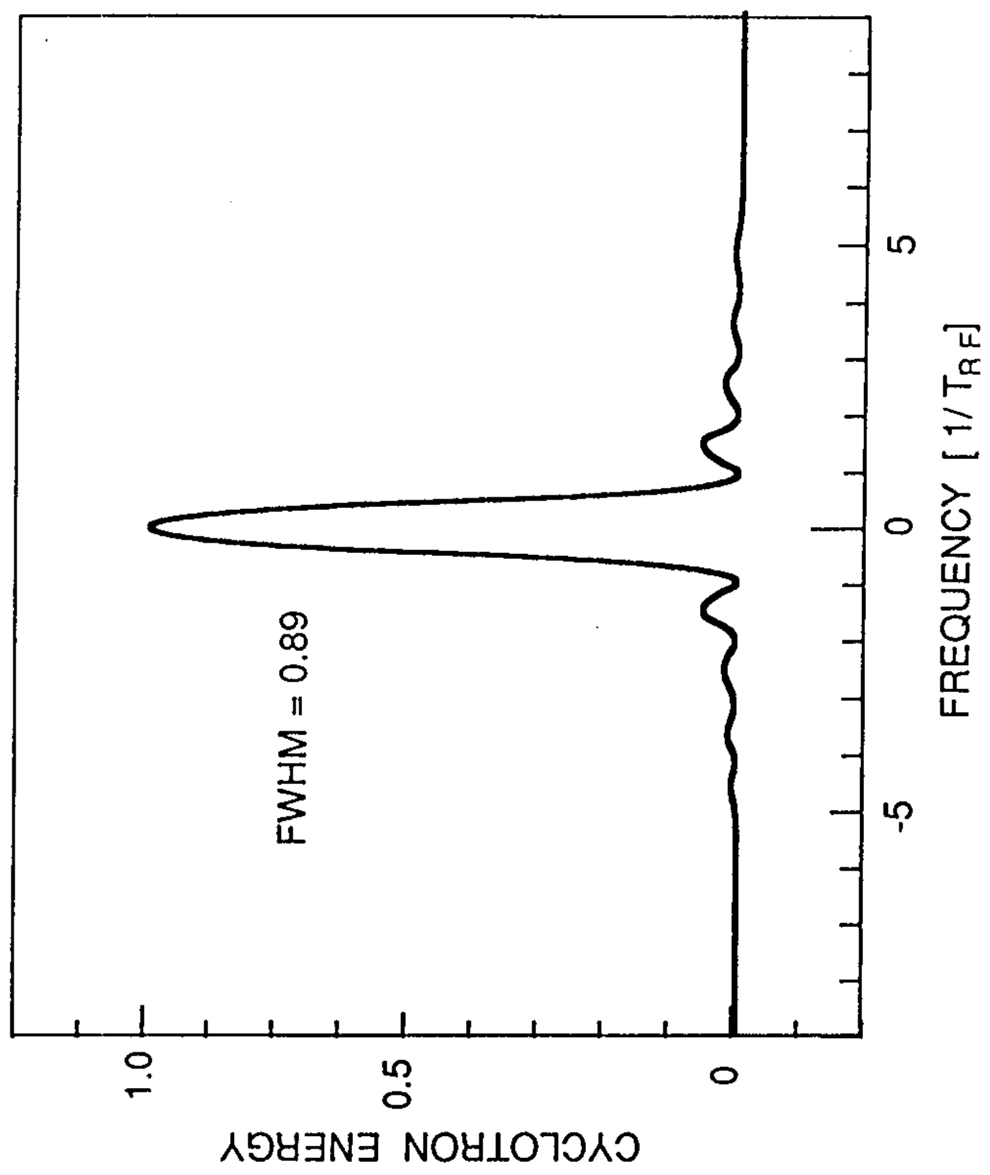

Figure 3.

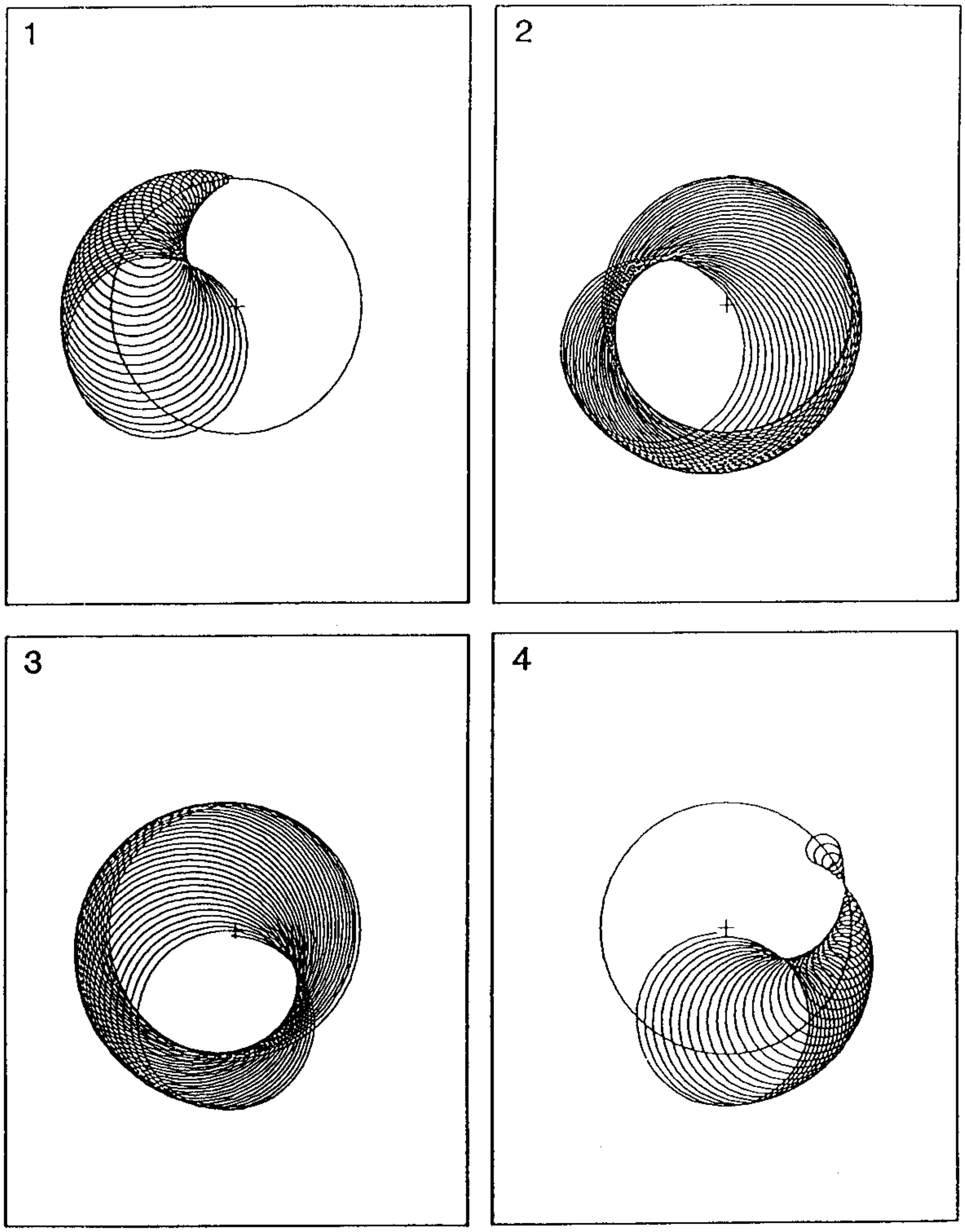

Figure 4.

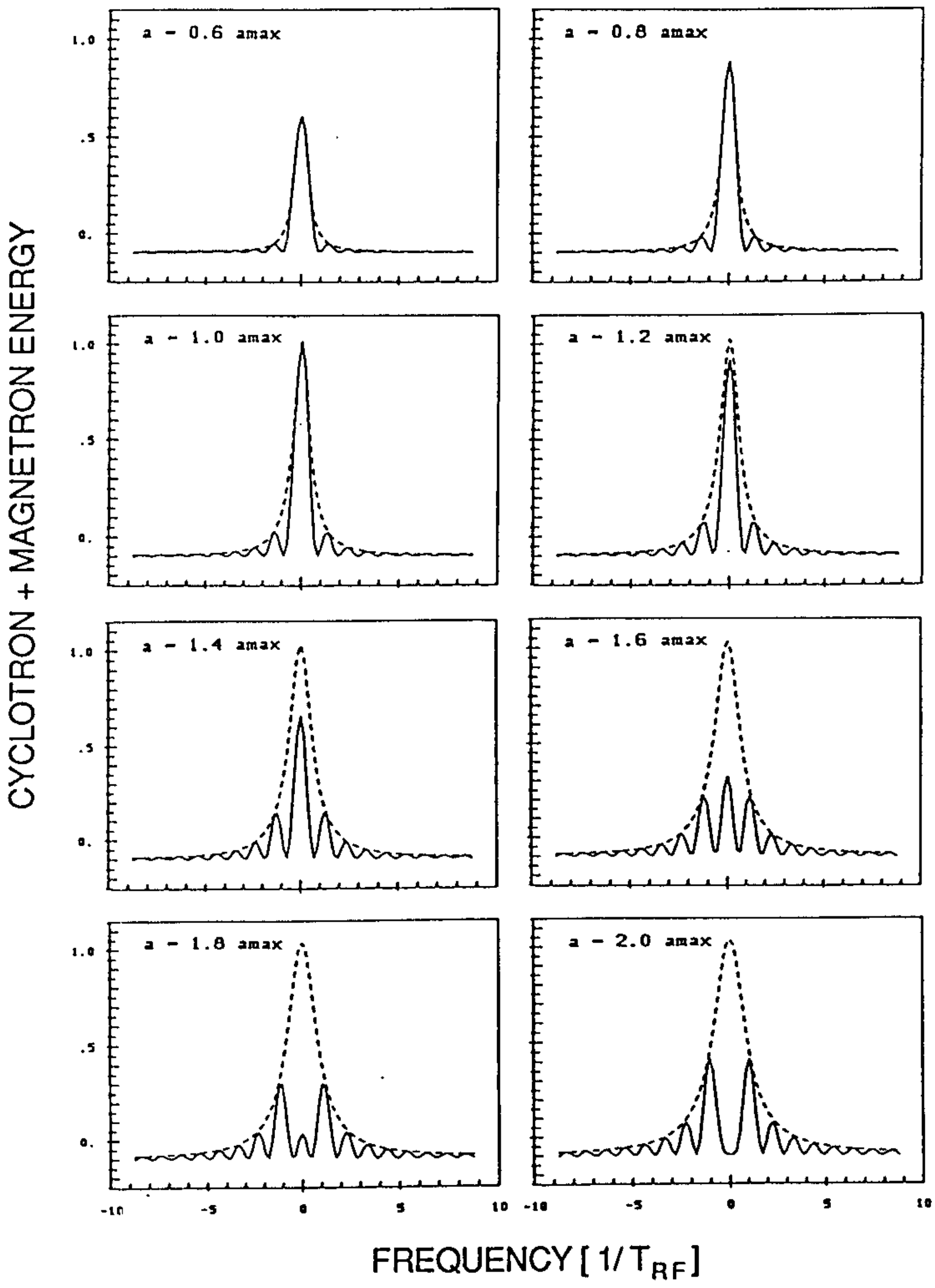
a = 0.6 amax
a = 0.8 amax
a = 1.0 amax
a = 1.2 amax
a = 1.4 amax
a = 1.6 amax
a = 1.8 amax
a = 2.0 amax
1.0
.5
0.
-10
-5
0
5
10
CYCLOTRON + MAGNETRON ENERGY
FREQUENCY [1/ T_RF]

Figure 5.

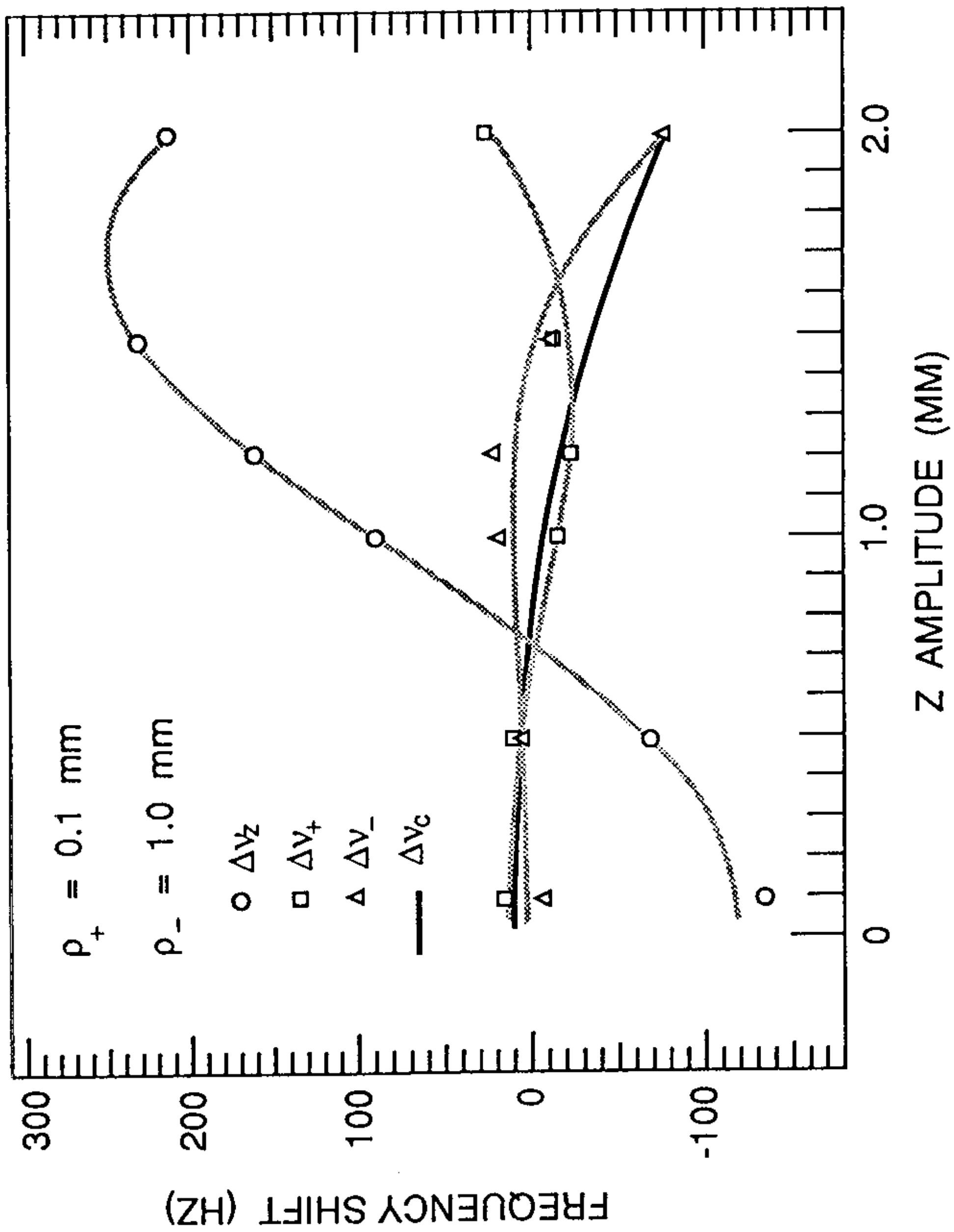

ρ_+ = 0.1 mm
ρ_- = 1.0 mm
$\Delta\nu_z$
$\Delta\nu_+$
$\Delta\nu_-$
$\Delta\nu_c$
300
200
100
0
-100
FREQUENCY SHIFT (HZ)
0
1.0
2.0
Z AMPLITUDE (MM)

Figure 6.

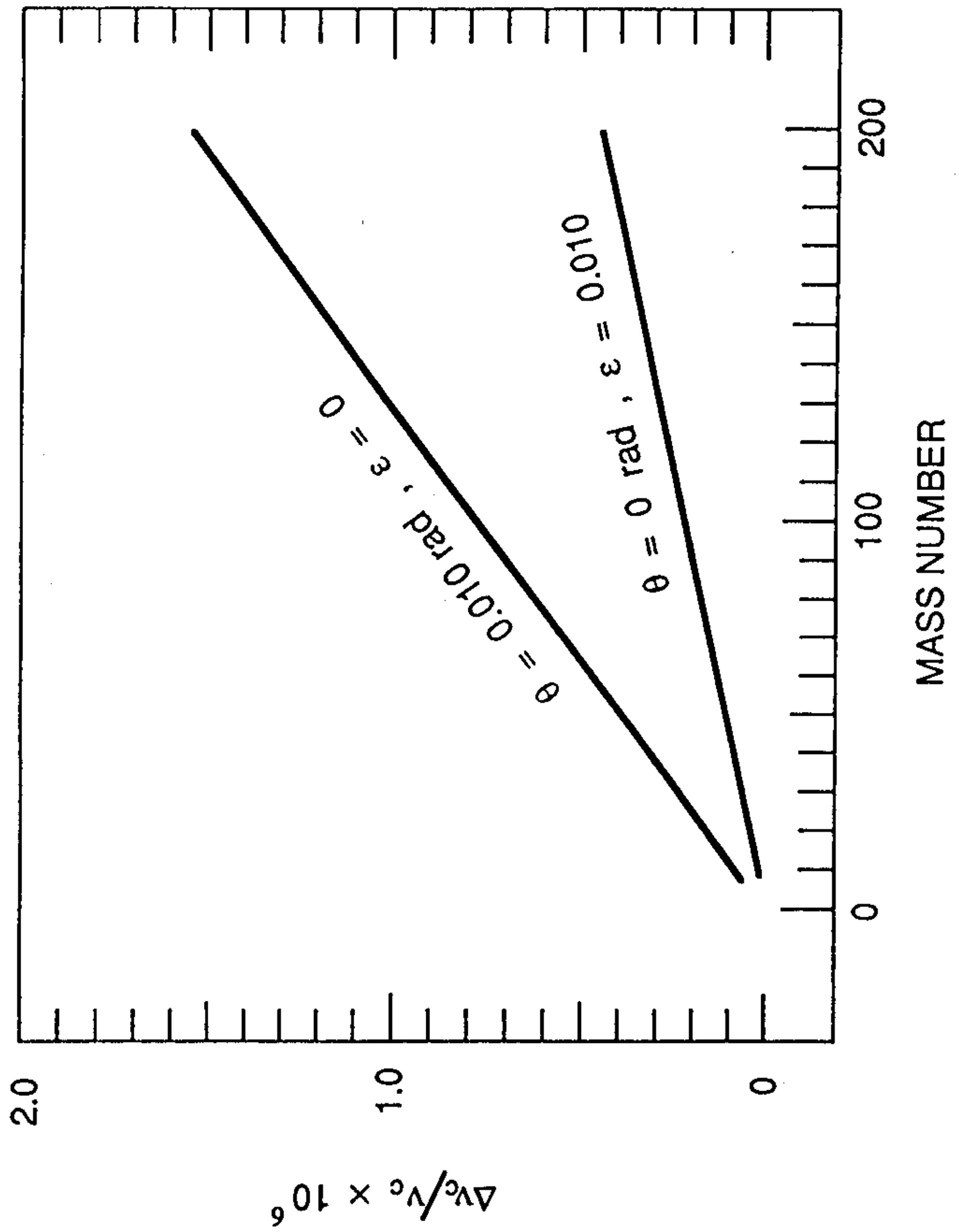
θ = 0.010 rad , ε = 0
θ = 0 rad , ε = 0.010
MASS NUMBER
0
100
200
2.0
1.0
0
Δν_c/ν_c × 10^6

Figure 7.

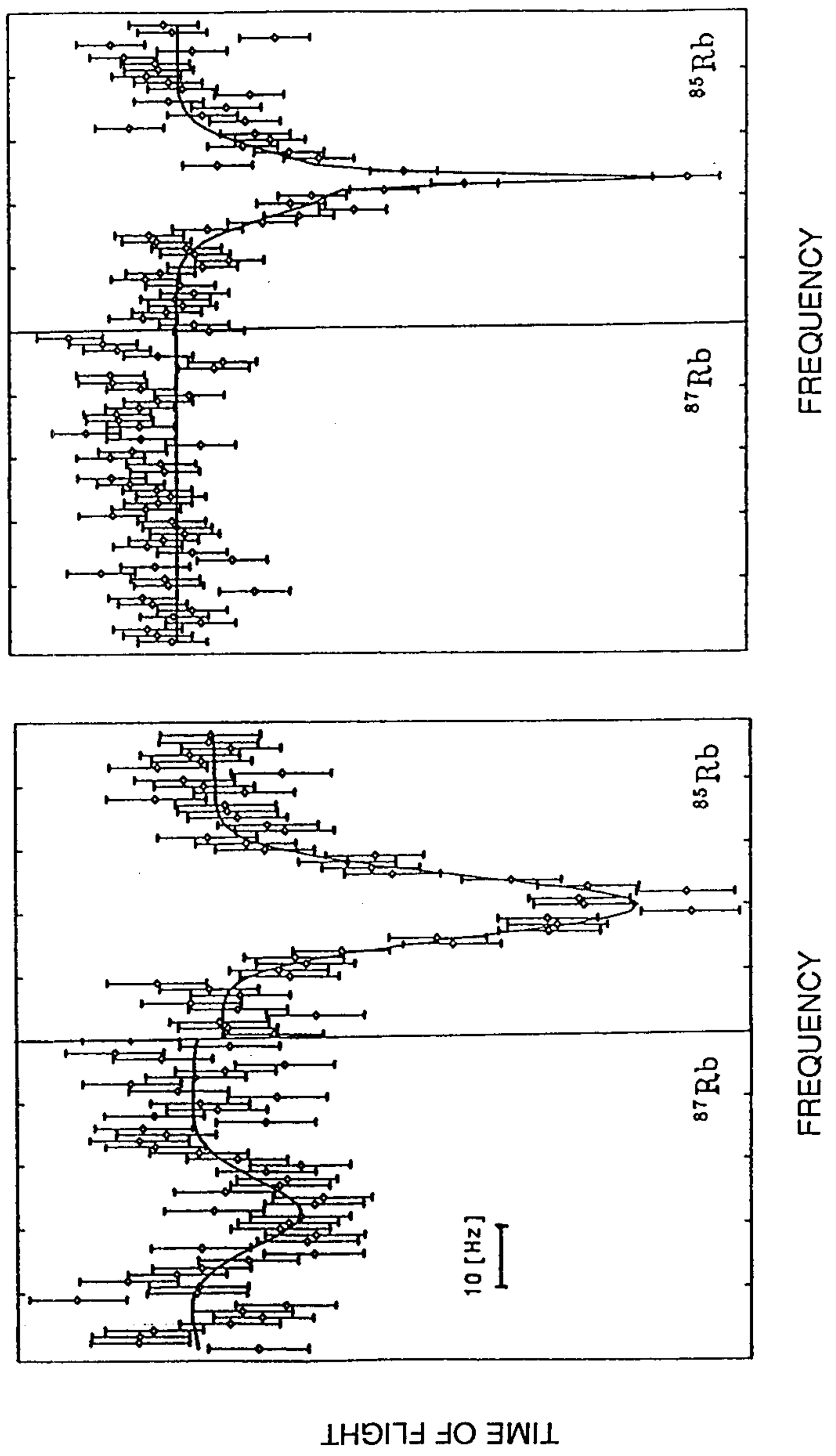
^{85}Rb
^{87}Rb
FREQUENCY
^{85}Rb
^{87}Rb
10 [Hz]
FREQUENCY
TIME OF FLIGHT

Figure 8.

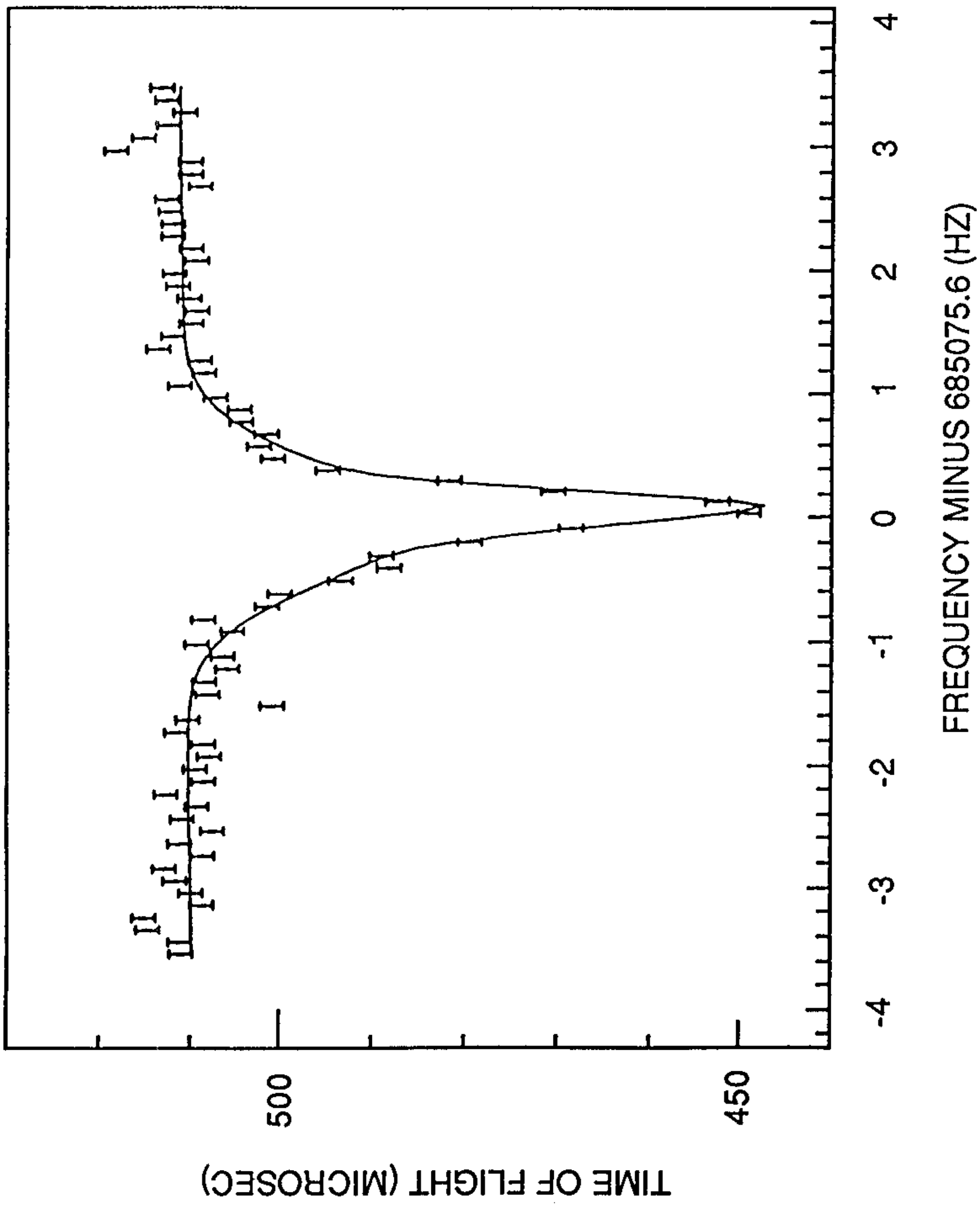

TIME OF FLIGHT (MICROSEC)
500
450
FREQUENCY MINUS 685075.6 (HZ)
-4
-3
-2
-1
0
1
2
3
4

Figure 9.

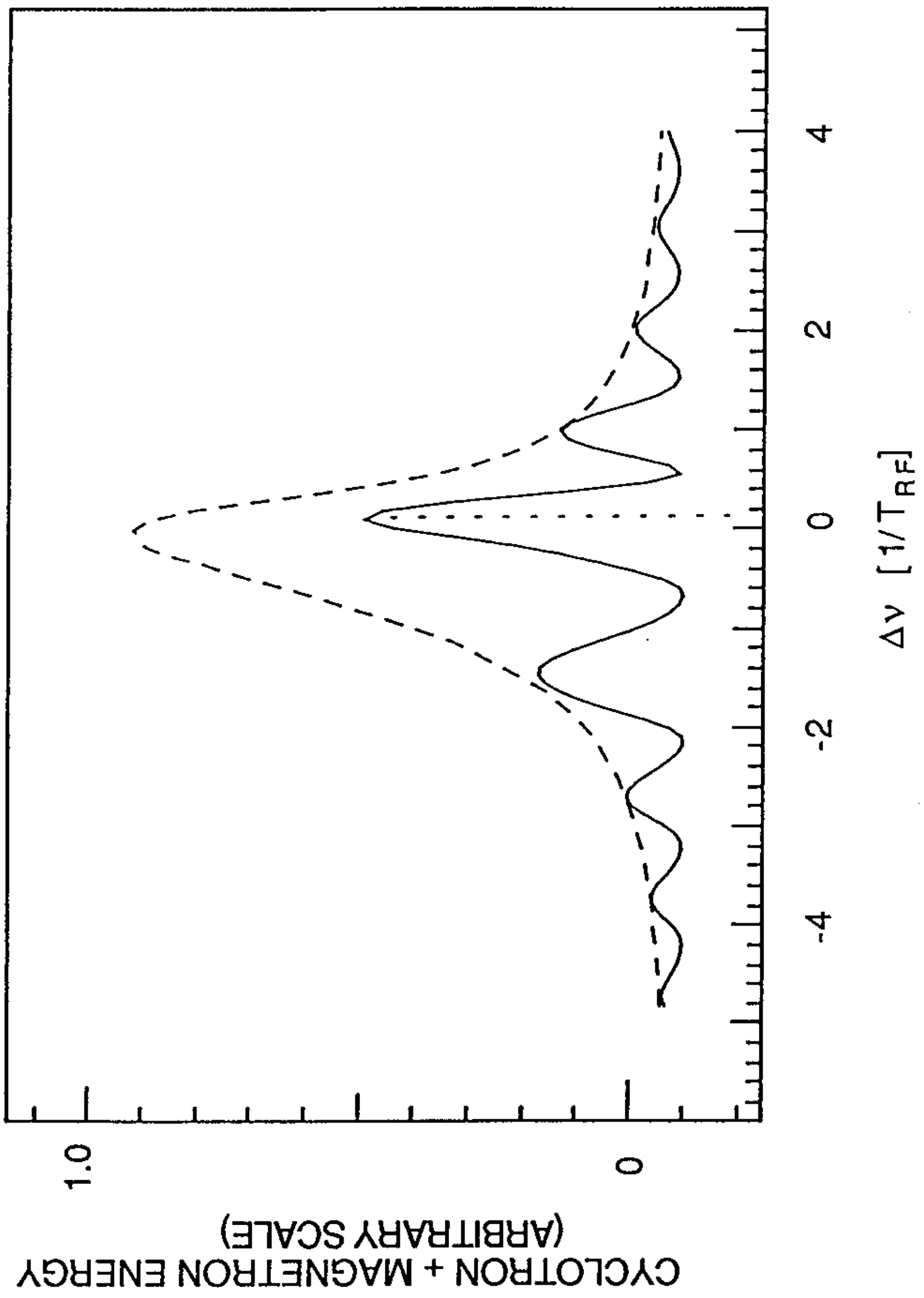
CYCLOTRON + MAGNETRON ENERGY
(ARBITRARY SCALE)
1.0
0
-4
-2
0
2
4
Δν [1/T_RF]

Figure 10.

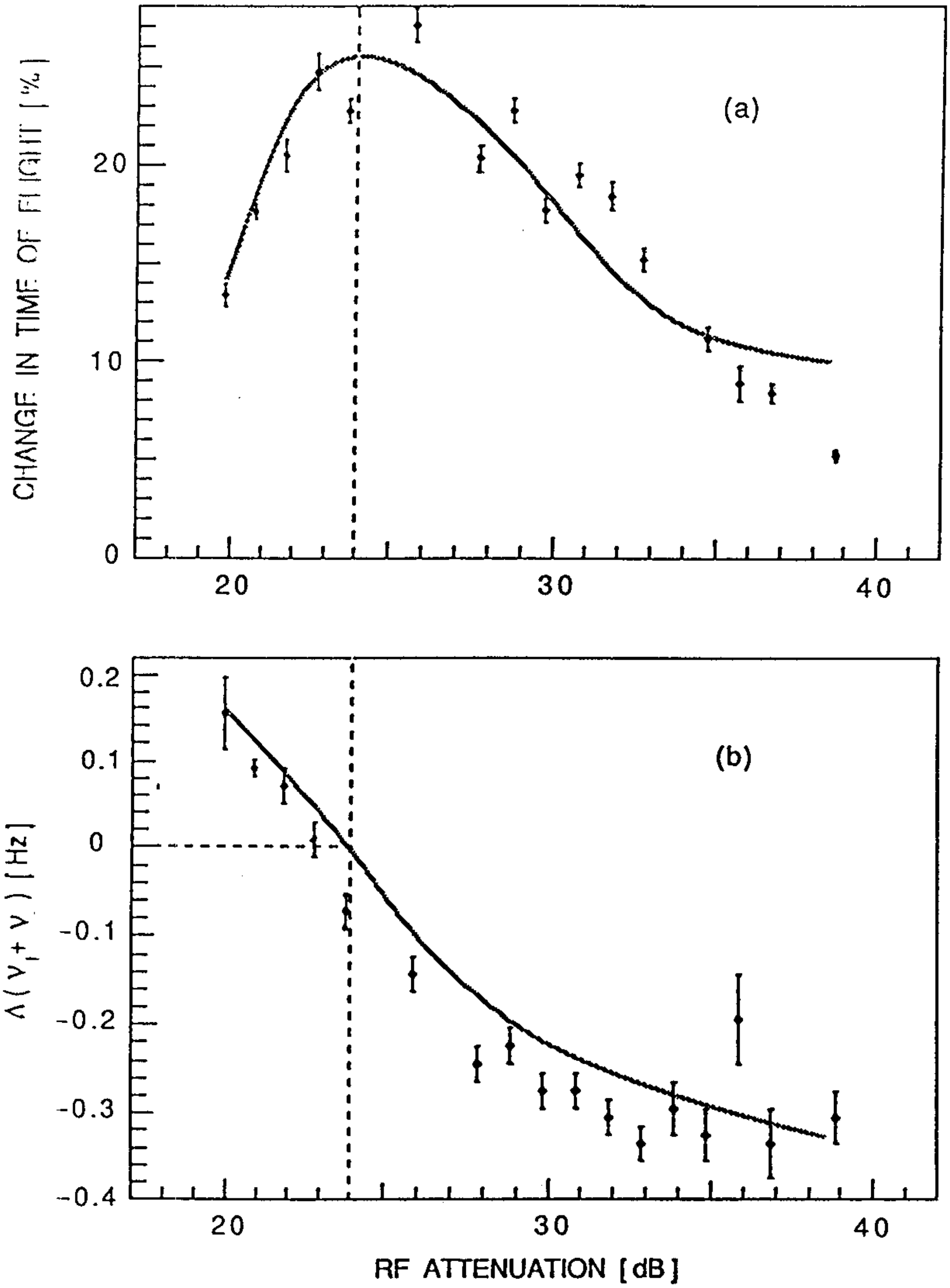
(a)
CHANGE IN TIME OF FLIGHT [%]
0
10
20
20
30
40
(b)
Δ(ν+ + ν-) [Hz]
0.2
0.1
0
-0.1
-0.2
-0.3
-0.4
20
30
40
RF ATTENUATION [dB]

Figure 11.

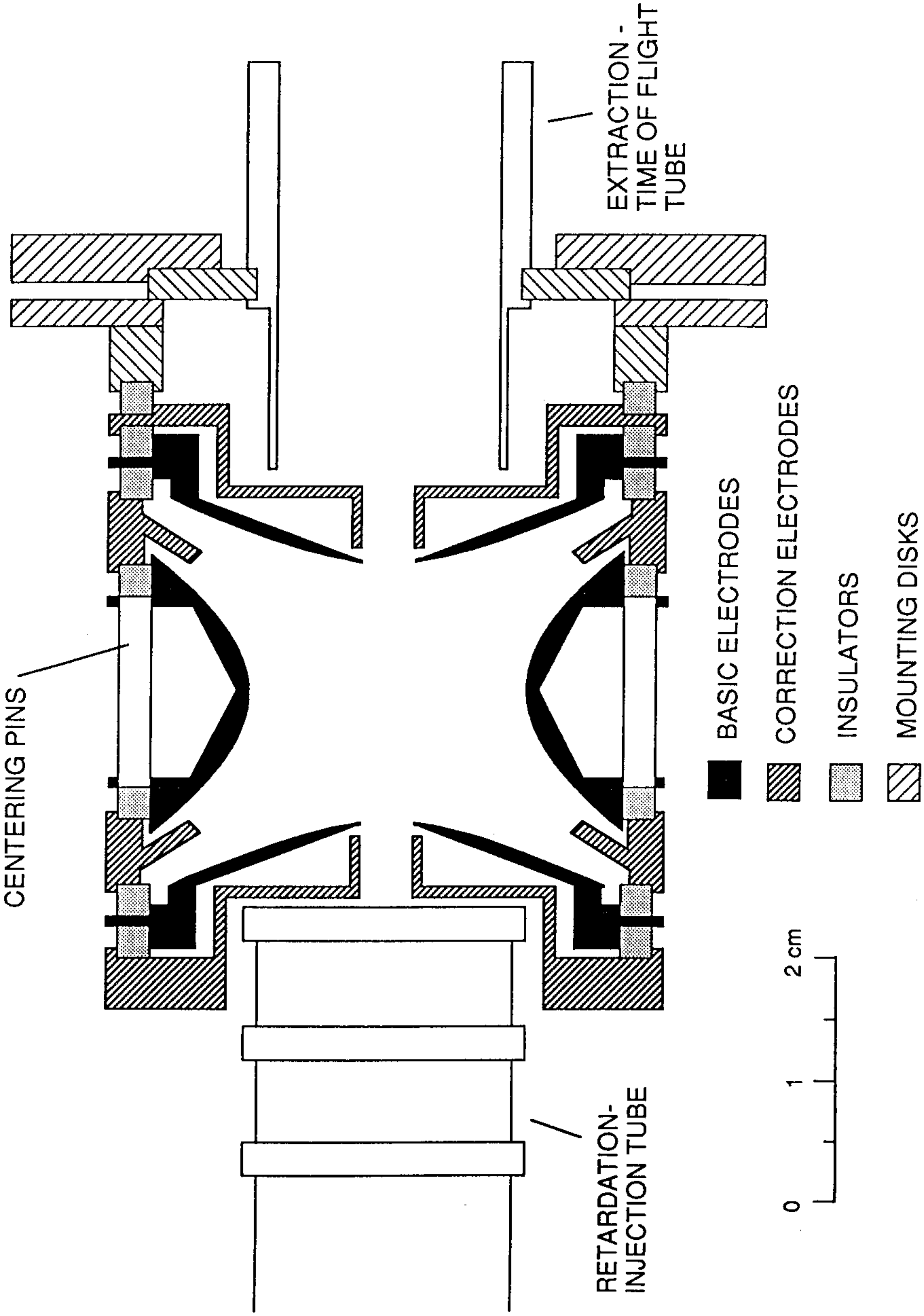
EXTRACTION -
TIME OF FLIGHT
TUBE
CENTERING PINS
BASIC ELECTRODES
CORRECTION ELECTRODES
INSULATORS
MOUNTING DISKS
RETARDATION-
INJECTION TUBE
2 cm
1
0